UNIVERSITY OF HELSINKI
FACULTY OF SCIENCE
DEPARTMENT OF PHYSICS

REPORT SERIES IN GEOPHYSICS

No 74

Cover: (Emperor penguin in Rampen, Photograph by O. Järvinen).

ANNUAL CYCLE OF THE ACTIVE SURFACE LAYER IN WESTERN DRONNING MAUD LAND, ANTARCTICA

Onni Järvinen

HELSINKI 2013

ISBN 978-952-10-8932-9 (printed version)
ISSN 0355-8630
Helsinki 2013
Yliopistopaino

ISBN 978-952-10-8933-6 (pdf-version)
Helsinki 2013
http://ethesis.helsinki.fi

ANNUAL CYCLE OF THE ACTIVE SURFACE LAYER IN WESTERN DRONNING MAUD LAND, ANTARCTICA

Onni Järvinen

ACADEMIC DISSERTATION IN GEOPHYSICS

To be presented, with the permission of the Faculty of Science of the University of Helsinki for public criticism in the Auditorium A110 of Chemicum, A.I Virtasen aukio 1, on September 27th, 2013, at 12 o'clock noon.

Contents

Nomenclature

AWS	=	automatic weather station
BIA	=	blue ice area
d	=	day
D	=	depth of the pump hole
DML	=	Dronning Maud Land
ER_{ds}	=	erosion/deposition due to divergence/convergence of the horizontal snowdrift transport
$F_{\downarrow}$	=	downwelling planar irradiance
$F_{\uparrow}$	=	upwelling planar irradiance
G	=	subsurface energy flux including surface melt
k	=	diffuse extinction coefficient
k_t	=	thermal conductivity
K	=	hydraulic conductivity
K_a	=	ice-air heat exchange coefficient
L	=	latent heat of freezing
LWC	=	liquid water content
ME	=	melt
m.a.s.l.	=	metres above sea level
PAR	=	photosynthetically active radiation (400–700 nm)
PR	=	solid precipitation
Q_H	=	turbulent flux of sensible heat
Q_{LE}	=	turbulent flux of latent heat
Q_{LW}	=	net longwave radiative flux
Q_{SW}	=	net shortwave radiative flux
r	=	distance from the centre of the hole
r_0	=	radius of the pump hole
S	=	sum of freezing-degree-days
S.D.	=	standard deviation
SMB	=	surface mass balance
SU_{ds}	=	sublimation of drifting-snow particles in a column extending from the surface to the top of the drifting-snow layer
SU_s	=	surface sublimation/deposition
t	=	time
T	=	transmittance
T_a	=	air temperature
T_m	=	mean air temperature
V	=	discharge rate in pumping
w.e.	=	water equivalent
α	=	albedo
$\epsilon(\lambda)$	=	e-folding depth
λ	=	wavelength
ξ	=	water surface level

This thesis is based on the following five articles, which are referred to in the text by their Roman numerals:

Paper I: Järvinen, O. and M. Leppäranta. 2011. Transmission of solar radiation through the snow cover on floating ice. *Journal of Glaciology*, **57**(205), 861–870.

Paper II: Leppäranta, M., O. Järvinen and O.-P. Mattila. 2012. Structure and life cycle of supraglacial lakes in the Dronning Maud Land. *Antarctic Science*, available on CJO2012. doi:10.1017/S0954102012001009.

Paper III: Järvinen, O. and M. Leppäranta. 2013. One-year records from automatic snow stations in western Dronning Maud Land, Antarctica. *Antarctic Science*, available on CJO2013. doi:10.1017/S0954102013000187.

Paper IV: Järvinen, O. and M. Leppäranta. 2013. Solar radiation transfer in the surface snow layer in Dronning Maud Land, Antarctica, *Polar Science*, **7**(1), 1–17. http://dx.doi.org/10.1016/j.polar.2013.03.002.

Paper V: Leppäranta, M., O. Järvinen and E. Lindgren. 2013. Mass and heat balance of snow patches in Basen nunatak, Dronning Maud Land in summer, *Journal of Glaciology*, submitted in December 2012.

Abstract

Antarctica is a major component in the climate system of the earth, acting as a large heat sink in the energy balance. The climatic conditions of Antarctica maintain the snow and ice cover that blankets almost completely the surface area of the continent. Physical properties of snow readily respond to changing environmental conditions and remote sensing signals are sensitive to these properties. The annual changes in the physical properties of the snow cover, especially in the coastal area, must be taken into account when snow cover and climate models are produced. In situ observations are needed for calibration and validation of these models.

The aim of the present study was to examine the annual cycle of the active 10-m surface layer in western Dronning Maud Land, Antarctica. The data were collected along a 300-km-long transect from the coast to the edge of the high plateau during the field campaigns in austral summers 2004–2005, 2009–2010 and 2010–2011 as a part of the Finnish Antarctic Research Programme (FINNARP). The studies were focused on the uppermost part of the ice sheet covering the most recent annual accumulation in the coastal area.

The results showed that the present study lakes froze completely during winter and showed similar evolution but the exact timing depended on the location. In January, the general structure of lake Suvivesi was following: two layers, each about 1 m thick, an upper layer with a thin ice layer on top and main body of liquid water, and a lower layer containing slush and hard ice sub-layers. The formation and the depth scale of the present study lakes are determined by the light extinction distance and thermal diffusion coefficient, limiting the growth to less than $\sim$1.5 m in one summer. In Antarctica, the mean spectral diffuse extinction coefficient varied between 0.04 and 0.31 cm^{-1} (10–20-cm snow layer) and varied only slightly between locations when the grain type was the same. The theoretically calculated average depth where broadband irradiance (400–700-nm band) was 1 % of the downwelling irradiance at the surface, was 50 cm. On the continental ice sheet, the compaction rate of the snowpack was 0.0201 $\pm$ 0.02 y^{-1} and the power spectra revealed a daily cycle, synoptic scale variability ($\sim$10 days), and variability in a low-frequency band of 60–120 days at a depth of 54 cm. The investigations of snow patches in Basen nunatak revealed that much more snow was lost in summer 2010–2011 (6.3 mm d^{-1} water equivalent (w.e.)) than in 2004–2005 (4 mm d^{-1} w.e.).

Acknowledgments

Even the ancient Phoenicians were famous for exploring the world. In their footsteps I have been given a chance to travel to the edge of the world and play with snow. These snow measurements and this thesis would never have become reality and never been completed without the help of several people and groups. I would like to thank these people and groups for their support and assistance during my studies:

I thank my supervisor Professor Matti Leppäranta for giving me the opportunity to work in the Division of Geophysics and Astronomy and in the Antarctica project. He has given me a lot of independence and liberty with my research. It was a privilege to travel with Matti to Antarctica and watch the television series "Kummeli" after a long day of field work.

Juho Vehviläinen is responsible for building the snow stations. He was an excellent travelling company during the first Antarctica expedition in 2009. We had a lot of fun in Antarctica and these memories I cherish.

I also want to thank adjunct Professor Esko Kuusisto and Professor Timo Vihma for providing critical and constructive comments while reviewing the manuscript of the thesis. Their comments have been crucial.

The Department of Physics/Division of Geophysics and Astronomy provided the working facilities. The Finnish Antarctic Research Programme (FINNARP) was responsible for logistics to Antarctica. I want to thank the members of the FINNARP 2009 and 2010 expeditions. Special thanks go to expedition leaders Petri Heinonen and Mika Kalakoski. This work was funded by the Academy of Finland (project No. 122787 and 127691).

I want to thank my parents for their support throughout my life. Their support has been crucial. I thank my friends for asking fascinating and important questions related to snow, e.g. "*Can you eat yellow snow?*". These inquiries have helped me to become a competent snow scientist and as my good friend says: "Lumitutkija on nietoksissa."

1. Introduction

Snow and ice covers 98 % of all surfaces in Antarctica which form a major component in the climate system of the earth due to its size, high latitude and freshwater storage (Bindschadler, 1998). These enormous ice sheets result in strong radiative heat losses, and there is close interaction between the radiation climate and boundary-layer dynamics (Van den Broeke, 2004a). Antarctica also provides a unique environment to study the snow cover, because it has the cleanest atmospheric environment available on Earth (Legrand and Mayewski, 1997). Additionally, Antarctica is the coldest, windiest, and driest continent and has the highest average elevation of all the continents (King and Turner, 1997).

Mass balance of the Antarctic ice sheet regulates the mean global sea-level elevation (Rignot and Thomas, 2007). Studying the spatiotemporal variations in the physical properties of the Antarctic snow cover is crucial because the surface of the ice sheet is formed almost completely of snow, which easily responds to changes in environmental conditions. The buried individual snow layers transform into ice and record past weather and climate conditions in terms of local temperature, precipitation, and aerosol fluxes of marine, volcanic, terrestrial, cosmogenic and anthropogenic origin (Petit et al., 1999). The net accumulation rate and the variability of the surface environment are crucial for snow cover and climate models in Antarctica (e.g. Van Lipzig et al., 2002a,b; Liston and Elder, 2006). These models are the key to understand the current and past relationships between the global climate and the Antarctic ice sheet.

The surface solar radiation budget is dominated by the high albedo of the snow cover, and even small changes in the albedo cause large relative changes in the amount of radiation absorbed. Observations in western Dronning Maud Land (DML) show that the albedo varies between 0.8 and 0.9 for dry snow in clear sky conditions (e.g. Pirazzini, 2004), and for wet snow the albedo is from 0.7 to 0.8 (Kärkäs et al., 2002). The snow cover is weakly transparent to sunlight, and therefore in summer the solar radiation heats the upper 0.5-m layer of the snow cover. Thus, light transfer in snow is a major issue in the snow energy balance, particularly in melting snow, because the optical properties are sensitive to the liquid-water content (LWC). The presence of liquid meltwater lowers the albedo and melting thus boosts a positive feedback. Parameterization of the radiation transfer is important in snow thermodynamic models.

Scattering and absorption determine light transmittance in a snowpack and are dependent on a combination of snow properties and light conditions. In a snowpack, there is a multitude of optically different layers, such as depth/surface hoar and ice lenses. Transmittance is expected to fall exponentially with depth, but close to the surface there is a transition zone where irradiance is not yet diffuse and stronger attenuation is found (Beaglehole et al., 1998). In the transition zone, the transmittance is dependent on a combination of solar elevation,

snow stratigraphy, scattering and absorption coefficients, and wavelength. The wavelength determines the direct/diffuse ratio of the incident downwelling irradiance at the surface (Lee-Taylor and Madronich, 2002). Direct solar radiation predominates over diffuse radiation under clear skies (Baker et al., 1999).

In blue ice areas (BIAs), the surface layer is free of snow and ice is visible. The formation of BIAs is initiated by a divergence in the transport of drifting snow, either by blocking of a nunatak or by wind erosion. At BIAs, the ablation by sublimation and possibly wind scouring exceeds the accumulation; precipitation and snowdrift deposition. Thus, the surface mass balance of BIAs is negative. BIAs are scattered widely over the Antarctic continent and exist even in the coldest parts yet covering only approximately 1 % of the ice sheet. An important feature of blue ice is its relatively low albedo (0.56–0.69) compared with that of dry snow (0.8–0.9) indicating that blue ice absorbs approximately twice as much solar radiation as snow (Bintanja, 1999).

Supraglacial lakes are known to form in BIAs due to the low albedo. They form in the surface layer of the BIA in summer due to penetration of solar radiation into the ice. Supraglacial lakes influence the local heat budget by their increased capacity to absorb solar radiation. These lakes feed liquid water into fractures in the ice sheet, and show sensitivity to climatic conditions and thereby assist detection of regional climate change (e.g. Winther et al., 1996).

Nunataks are striking features in the Antarctic landscape puncturing the ice sheet and raising high above it, even several thousand metres. Their surface contains bare areas, seasonal and perennial snow patches, and small glaciers. The zero snow mass balance (accumulation = ablation) of the seasonal snow patches is due to wind transport of snow, sublimation, and summer melting. The melt waters from snow patches are the source of moisture for the soil, and they may form drainage systems, which contain liquid water ponds with specific ecosystems where phytoplankton has been found (Keskitalo et al., 2013). The small nunatak glaciers may contain very old ice since net accumulation of snow may be very slow. The influence of climate variations should show up clearly in the snow mass balance of nunataks.

The present study concerns the annual cycle of the active 10-m surface layer in western DML and is a part of the *'Evolution of snow cover and dynamics of atmospheric deposits in the snow in the Antarctica'* project that belonged to the consortium *'Antarctic coastal and high plateau aerosols and snow'* led by the Finnish Meteorological Institute. The project was performed in 2009–2012, and it was a continuation to earlier snow research programme *'Seasonal snow cover in Antarctica'* (1999–2005) (Rasmus et al., 2003). The general strategy was to get detailed knowledge of the physical properties of the 10-m surface layer and of the factors responsible for producing them in the research area covering a 300-km deep sector in the DML. The specific objectives of the present study were to 1) examine the spatial variation of the physical properties of snow and to acquire additional snow pit data, 2) determine the annual snow accumulation and ablation rates and their spatial variations, 3) measure the optical properties of the surface layer, and 4) examine the life history of supraglacial and epiglacial lakes.

Here is presented a short summary of the results of the present study. The three study lakes showed similar evolution, although summer was warmer in 2010–2011 than in 2004–2005. The exact timing of evolution depended on the

location and all three lakes froze completely during winter. In January, the general structure of lake Suvivesi was following: the lake body consisted of two layers, each about 1 m thick, an upper layer with a thin ice layer on top and main body of liquid water, and a lower layer containing slush and hard ice sub-layers. The warmer summer in 2010–2011 was also noticed in the heat and mass balance investigations of snow patches in Basen nunatak.

1.1 Author's contribution

The author's own contribution to each publication is mentioned below and presented separately.

Paper I: Onni Järvinen is responsible for the measurements on the field, data analysis and figures. Writing of the article was done together with Matti Leppäranta. Total contribution of Onni Järvinen is 75 %.

Paper II: Onni Järvinen took part in the field measurements during the second field season, 2010–2011. Onni Järvinen took also part in writing and produced figures to the article. Total contribution of Onni Järvinen is 35 %.

Paper III: Onni Järvinen took part in installing and retrieving the snow stations. Onni Järvinen is responsible for the data analysis and figures. Writing of the article was done together with Matti Leppäranta. Total contribution of Onni Järvinen is 70 %.

Paper IV: Onni Järvinen is responsible for the measurements on the field, data analysis and figures. Writing of the article was done together with Matti Leppäranta. Total contribution of Onni Järvinen is 75 %.

Paper V: Onni Järvinen carried out some of the field measurements during the second field season, 2010–2011. Onni Järvinen took also part in writing and produced figures to the article. Total contribution of Onni Järvinen is 40 %.

2. Glaciophysical properties of the snowpack

2.1 Physical properties of snow

Snowpack is composed of ice crystals, air, water vapour, and sometimes liquid water and is a fine-grained material with a high specific surface area. A snowpack can be considered as a cellular form of ice, in which the individual ice crystals are bonded together. Cellular solids can be divided into a closed cell (e.g. soap foam) and an open cell (e.g. sponge) forms. Snow is classified as the open cell type where individual ice particles bond in linear chains forming an open cell polyhedral-type structure (Petrovic, 2003). The purpose of this section is not to provide a complete review of the physical properties of snow, but to list the quantities relevant to the present study.

2.1.1 Density

Density is an important property of any material. In porous media, density generally refers to the bulk density, which is the total mass per volume. Most common method to determine snow density is weighing snow of a known volume. Although snow density is a bulk property, an accurate value is necessary for microstructure based studies. In nature, snow density varies greatly due to local meteorological conditions; density of a freshly fallen snow can be as low as 50 kg m^{-3} and a wind packed snow is in the range of 300–400 kg m^{-3}. If the snow density keeps increasing, snow will eventually transform into ice. This occurs when the snow density reaches a value of 830 kg m^{-3} and the air pores have encapsulated air bubbles (e.g. Paterson, 1994). Further densification occurs by compression of the air bubbles. In glaciers, the transformation of snow into ice is much more rapid in a wet-snow zone than in a dry-snow zone. In the dry-snow zone snow transforms into ice when depth is approximately 60 to 70 m (Paterson, 1994). The transformation of snow into ice under pressure is a very slow process unless meltwater is present.

Compaction (densification) of snow is an important parameter especially in the field of remote sensing. In Antarctica, compaction lowers elevation of the snow cover and this might be interpreted as loss of mass although the change in the elevation is due to the compaction. Densification of snow can be influenced by many different external conditions, particularly in the upper part of snowpack; e.g. wind-packing, sublimation, melting and freezing may cause a temporary increase or decrease in snow density (Kojima, 1964). Compaction of the snow occurs in two stages. First, there is an initial period of settlement where the

rate of volume decrease is dominated by thermal processes, reflecting the rapid metamorphism as branched crystals break down. The first stage is followed by a slower compaction as pores collapse, which is largely caused by the overburden (Gray and Morland, 1995).

2.1.2 Temperature

Thermal conductivity is an important physical property of snow and it determines the temperature gradient, and therefore affects the rate of snow metamorphism. Thermal conductivity is a function of snow structure (e.g. grain size and shape, and bonding) and density (Sturm et al., 1997). The thermal conductivity of snow is low and difficult to measure (Riche and Schneebeli, 2012). In glaciers, the mean annual air temperature at the surface can be estimated to be same as the snow temperature measured at a depth of 10 m. The accuracy of this estimation depends on the structure of the snow, how the air temperature varies within the year and are there changes in the long term air temperature. Within an ice sheet, thermal energy (heat) is transferred primarily by conduction but in some cases other heat transfer mechanisms must also be taken into account. Nonconductive processes include wind-generated ventilation of the snowpack (wind-pumping), latent heat transfer by water-vapour migration, convection of air in the pore spaces and solar radiative heating. These processes are limited to the uppermost few metres of snow (Brandt and Warren, 1997).

Rusin (1961) reported a temperature maximum at the depth of about 10 cm in cold Antarctic snow during summer, but not all snow temperature measurements agree with Rusin (e.g. Carrol, 1982). The temperature maximum probably existed even though the radiative heating of thermistors caused an increase to the measured sub-surface temperatures by Rusin (Brandt and Warren, 1993). In western DML, the temperature profiles in the uppermost 0.30 m strongly depend on the cloud conditions, which control the downward radiative fluxes with opposite effects on solar shortwave and thermal longwave radiation (Vihma et al., 2011). Internal heat fluxes in wet snow are controlled by conduction and latent heat release due to freezing.

2.1.3 Grain size and shape

Grain size and shape changes (known as metamorphism) within the snow cover over the time, but the changes can also be very rapid and dramatic. Metamorphism is a continuous process that begins when the snow is deposited and continues until it melts. Rate of the metamorphism is closely related to the snow temperature. Below approximately -40 °C it practically comes to a stop (LaChapelle, 1969). A faceted form grows at expense of a rounded form when a large temperature gradient (at least 10–20 °C m^{-1}) is applied, while the rounded form grows at the expense of the faceted form when smaller temperature gradients occur (Colbeck, 1982). Both grain size and shape affect the snow density. Determination of grain shape and size is also crucial for validating snow models and interpreting remote sensing data (Lesaffre et al., 1998). In the field of remote sensing, grain sizes are sometimes used as an optical equivalent based on its scattering properties; optical grain size, effective grain radius and specific surface area (Wiscombe and Warren, 1980; Domine et al., 2008). There are sev-

eral methods for measuring and defining the grain size, but in this thesis the definition for the grain size is the greatest extension of the grain (measured in millimetres) and in terms from 'very fine' (size < 0.2 mm) to 'extreme' (size $>$ 5.0 mm) (Fierz et al., 2009).

Colbeck and other researchers collaborated in 1990 to develop an international classification for seasonal snow on the ground, dividing snow grains into nine different classes based on morphological features with additional information on physical processes and strength (Colbeck et al., 1990). A new revised classification was released in 2009 (Fierz et al., 2009) and the new classification is widely used in the field of snow research.

2.1.4 Liquid water content

Liquid water content (LWC) or free-water content is defined as the amount of water within the snow that is in the liquid phase. Liquid water in snow originates from either melt or liquid precipitation. It can also be a combination of the two. The LWC can be determined in field using a cold (freezing) or an alcohol calorimeter, the dilution method (Boyne and Fisk, 1990) and a snow fork (a complex permittivity, see 4. Methods). Measurements of LWC or wetness are expressed as either a volume or mass fraction. Both can be reported as percentages (%), which usually requires a separate measurement of density. Liquid water is mobile only if the residual or irreducible water content is exceeded. The irreducible water content is the water that can be held by surface forces against the pull of gravity (capillary action). Residual water content in snow corresponds to a volume fraction of about 3–6 %, depending on the snow type. A general classification of LWC follows as: dry 0 % (volume fraction), moist 0–3 %, wet 3–8 %, very wet 8–15 % and soaked $>$ 15 % (Fierz et al., 2009).

2.1.5 Impurities

Common impurities found in a snowpack are dust, sand, refractory black carbon (soot), acids, organic and soluble materials. Low amounts of impurities do not strongly influence the physical properties of snow but are of hydrological and environmental interest. Type and amount of impurities can be obtained by collecting snow samples in-situ and analysing them in a laboratory. Optically active impurities (other than air pockets) in the snowpack can significantly reduce visible and near-infrared reflectance and transmittance. Impurities in the snowpack are mainly absorbers and they lower the reflected radiation at their specific wavelengths (Warren and Wiscombe, 1980). In Antarctica, soot can be from the Antarctic stations or from low- and mid-latitudes and is deposited to the ice sheet preserving a history of emissions and atmospheric transport (e.g. Warren and Clarke, 1990; Bisiaux et al., 2012).

Studies have shown that the background levels of soot 10–13 km upwind of South Pole and Vostok stations were 0.1–0.3 ppb and 0.6 ppb, respectively. The peak values were found downwind of the stations (Warren and Clarke, 1990; Grenfell et al., 1994). The dust (clay minerals) content in the upper part of snowpack (modern snow) at the South Pole is approximately 15 ppb and 26 ppb at Dome C (Kumai, 1976; Royer et al., 1983). Soot is present in a lower concentration than dust (crustal origin), but it can dominate the absorption

because, for the sizes of soot and dust particles found in snow, soot is 50 times as absorptive as the same mass of dust (Warren, 1982; Warren and Wiscombe, 1980).

2.2 Optical properties of snow

Optical properties of material can be divided into apparent and inherent optical properties. The apparent optical properties depend on the directional distribution of incoming radiance in addition to the physical properties of the material. Inherent optical properties are independent of the incoming radiation. The material can be defined by three inherent optical properties: the absorption coefficient, the amount of absorption per unit distance; the scattering coefficient, the amount of scattering per unit distance; and the phase function, the angular dependence of scattering (Perovich, 2007).

The purpose of this section is not to provide a complete review of the optical properties of snow, but to list the quantities and equations relevant to the present study. This terminology is widely used, e.g. Perovich (2007). Here upwelling planar irradiance is $F_{\uparrow}$ and downwelling planar irradiance is $F_{\downarrow}$.

2.2.1 Albedo

Albedo, α, is the ratio of outgoing irradiance to incoming irradiance above the surface at a particular wavelength, λ (Warren, 1982). For the shortwave radiation (300–3000 nm), the albedo can be written as the ratio of spectrally integrated upwelling and downwelling irradiances at the surface:

$$\alpha = \frac{F_{\uparrow}(0^{-}, \lambda)}{F_{\downarrow}(0^{-}, \lambda)} \tag{2.1}$$

where 0^{-} refers to the level just above the snow surface. Broadband pyranometers are usually used to measure the irradiances integrated over the shortwave range. The albedo is probably the most significant and commonly measured optical property of the snow and is considered an apparent optical property. The albedo is basically straightforward to measure and calculate, but in practice there are several factors that affect the albedo and interpreting the albedo can be complicated. Wiscombe and Warren (1980) reported that at wavelengths where snow exhibits significant absorption, the albedo depends on the solar elevation with higher albedo at low solar elevations. This was also reported by Pirazzini (2004). Over a smooth, uniform and horizontal snow cover and under clear sky conditions, the albedo increases when the solar elevation decreases, since radiation incident at grazing angles has a larger probability of escaping from the snow grains without being absorbed, while radiation incident at larger angles penetrates deeper into the snowpack and is more likely trapped. When the solar elevation decreases the grain shape becomes more important and the albedo is higher, at low elevations, for more faceted grains (Choudhury and Chang, 1981).

The albedo decreases at all wavelengths as the grain size increases (Warren, 1982). The presence of liquid water in the snowpack causes an increase in the optically effective grain size. Thus, the albedo decreases when there is liquid water in the snowpack (Wiscombe and Warren, 1980). Cloud cover is normally

observed to cause an increase in the spectrally integrated albedo, but an exception can occur at very low solar elevations. The cloud cover absorbs the same near-infrared radiation that would normally be absorbed by the snow cover, leaving the shorter wavelengths (for which snow albedo is higher) to reach the snow surface and thus causing an increase in the albedo of snow. Basically the cloud cover changes the effective solar elevation converting direct radiation into diffuse radiation (Wiscombe and Warren, 1980).

2.2.2 Absorption

Absorption of radiation by ice is extremely weak at the visible and near-ultraviolet wavelengths, but in the near-infrared there are strong absorption bands. Between 300 and 600 nm the absorption is so weak that for some geophysical purposes it may as well be set to zero, for example, when computing absorption of solar radiation by ice clouds, because path lengths of photons through atmospheric ice crystals are very small compared to the absorption length (Warren et al., 2006). In this spectral range clean fine-grained snow reflects 97–99 % of the incident sunlight (Grenfell et al., 1994). The visible and near-visible region lacks absorption mechanisms for ice, as it lies between the electronic absorptions of the UV and the vibrational absorptions of the IR. The absorption coefficient increases with wavelength by five orders of magnitude across the solar spectrum from 500 to 2000 nm. Therefore the survival probability of photons in a snowpack after multiple-scattering events decreases substantially with wavelength (e.g. Warren et al., 2006). Due to extremely weak absorption at the visible and near-ultraviolet wavelengths small amounts of optically active impurities in snow can dominate the absorption of solar radiation at these wavelengths. Warren et al. (2006) reported that the absorption minimum for pure snow was 390 nm in Antarctica, but impurities in snow might have affected the result.

2.2.3 Scattering

At the visible wavelengths, snow is a highly scattering optical medium and the scattering predominates over the absorption (Warren, 1982). A snowpack has a multitude of air/ice interfaces to scatter light, but the basic scattering properties of snow are not well known and are difficult to measure directly. Most of the scattering is the result of change in direction of the light beam upon transmission through the grain, rather than reflection and the scattering coefficient is independent of wavelength across the visible and near-ultraviolet (Bohren and Barkstrom, 1974; Warren and Brandt, 2008). With a few simplifications, the scattering coefficient can in principle be calculated from fundamental scattering theory (e.g. Wiscombe and Warren, 1980). It can be simplified that in the visible and near-infrared wavelengths the scatterers are the snow grains, which are much larger than the wavelength, and the scattering is in the geometric optics regime. Also, the real portion of the index of refraction is assumed to have only little spectral variation in this wavelength region. Thus, the reflection coefficients are assumed to be also constant with the wavelength (Perovich, 2007). These calculations are complicated due to the large inherent variability in shape and composition of particles in a realistic snowpack. There are available radiative-transfer models that have been developed for snow to quantify the scattering

properties from radiation measurements (Bohren and Barkstrom, 1974; Warren and Wiscombe, 1980; Wiscombe, 1980; Wiscombe and Warren, 1980; Lee-Tayor and Madronich, 2002).

2.2.4 Light transmission

Transmittance (T) is the fraction of the downwelling planar irradiance ($F_{\downarrow}$) that is transmitted through the snow cover from the surface:

$$T = \frac{F_{\downarrow}(h, \lambda)}{F_{\downarrow}(0^{-}, \lambda)} \tag{2.2}$$

where h is depth, λ wavelength and 0^{-} refers to the level just above the snow surface. The transmittance is easy to calculate and provides the vertical distribution of the light spectrum in the snow cover. The transmittance is difficult to generalize, since it is strongly dependent on snow depth. Therefore, a quantity, e.g. extinction coefficient that is not dependent on the snow depth is needed.

The diffuse extinction coefficient (k) is normally calculated, using an irradiance attenuation law analogous to the Bouguer-Lambert absorption law (Warren, 1982):

$$\frac{dF_{\downarrow}}{dh} = -kF_{\downarrow} \tag{2.3}$$

The solution is

$$F_{\downarrow}(h, \lambda) = F_{\downarrow}(0^{+}, \lambda) \exp(-\int_{0}^{h} k(z)dz) \tag{2.4}$$

where 0^{+} refers to the level just below the snow surface. Equation (2.4) can be used to estimate the mean diffuse extinction coefficient between two measurement depths. The transmittance and diffuse extinction coefficient are both apparent optical properties. The inverse of the diffuse extinction coefficient equals the spectral e-folding depth $\epsilon(\lambda)$, which corresponds to the depth of the snow at which the diffuse irradiance has decreased by a factor of $1/e$ ($\sim$37 %).

3. Western Dronning Maud Land

The Antarctica studies were conducted in western DML in East Antarctica, covering a 300-km-long line from ice shelf edge to Heimefrontfjella mountain rage in the sector W011–017° (Fig. 3.1). The studies were conducted from the Finnish research station Aboa, located on the Basen nunatak (594 metres above sea level (m.a.s.l.)). The top of Basen is approximately 380 m above the surface of the neighbouring ice sheet. Basen is the most northern nunatak of the 130-km-long Vestfjella mountain range near the grounding line of the Riiser-Larsen Ice Shelf and the mountain range is aligned approximately parallel to the coast. In the Vestfjella area, the average altitude is approximately 400 m.a.s.l. and BIAs are common (Holmlund and Näslund, 1994). The Riiser-Larsen Ice Shelf north-west of Aboa floats and slopes gently from an elevation of slightly over 200 m near Aboa to < 50 m at the top of the shelf edge. The Heimefrontfjella mountain range is situated 150 km inland from Vestfjella and partly blocks the ice flow from the Amundsenisen plateau. The estimated large-scale surface slope at automatic weather station (AWS) 5 is 13.5 m km^{-1} and the ice shelf slopes seaward with a rate of typically 0.1 m km^{-1} (Van den Broeke et al., 2004b).

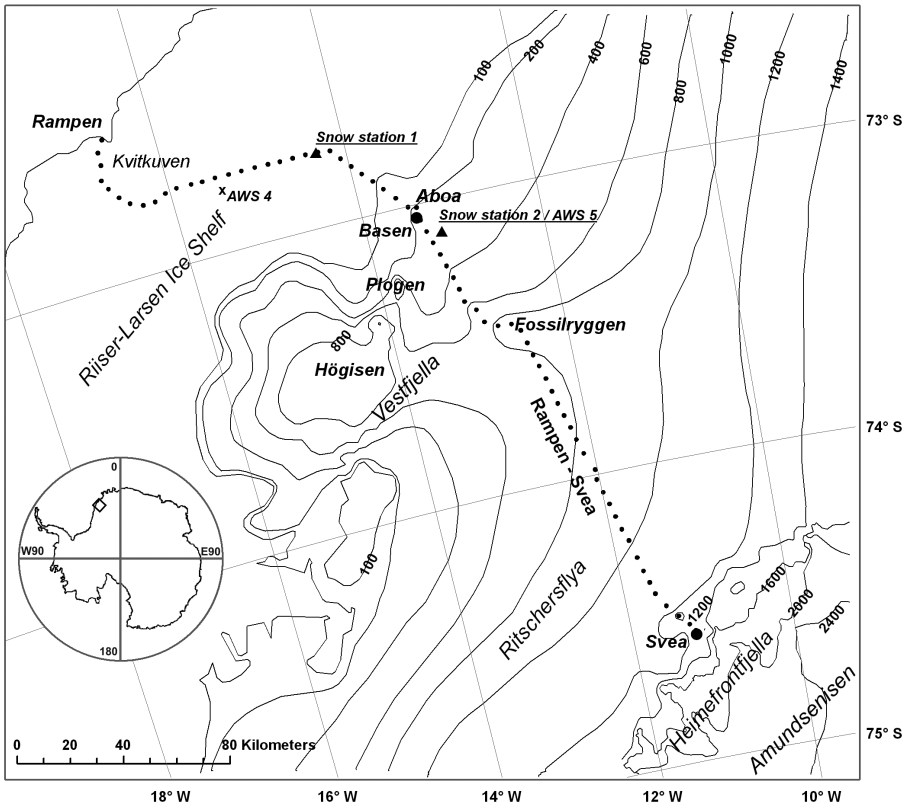

Figure 3.1: Map of the research area in western Dronning Maud Land.

The climate in the DML is determined by a combination of predominant katabatic winds and synoptic winds forced by transient cyclones traveling eastwards parallel to the coastline (Reijmer, 2001). The high elevation region behind Vestfjella mountain range is less affected by the changing sea ice cover and cyclonic activity than the coastal area (King and Turner, 1997). The cyclones bring moisture and impurities to the coastal zone of Antarctica and are responsible for most of the accumulation measured there (Tietäväinen and Vihma, 2008). The prevailing wind direction is from east–northeast (Reijmer, 2001). The annual mean 10 m wind speed on the ice shelf is 5.7 m s^{-1} and behind the grounding line on the continental ice sheet 7.8 m s^{-1}. The annual mean relative humidity is 93 % on the ice shelf, but on the continental ice sheet it decreases to 83 % (Van den Broeke et al., 2005).

The air temperature in western DML varies highly, especially in winter when the north-south and vertical temperature gradients are largest. Fluctuations of 20 to 30 °C within a few days are not unusual. In summer, AWS 4 and 5, and Aboa automatic weather station have recorded temperatures above 0 °C. The mean air temperature on the ice shelf is -19 °C, behind the grounding line -16 °C and on high elevation areas behind Vestfjella -20 °C (Reijmer and Oerlemans, 2002). Vihma et al. (2011) reported that in summer in the uppermost 0.2 m, the snow temperature correlated with the air temperature over the previous 6–12 h, whereas at the depths of 0.3 to 0.5 m the most important time scale was three days. Kärkäs (2004) reported that the monthly mean air temperature varied from -5.2 °C in January to -21.9 °C in August at the Aboa AWS (497 m.a.s.l) and the long-term (1989–2001) annual mean air temperature was -15.3 °C. The Aboa AWS provides air pressure, air temperature and humidity, wind speed and direction, and incoming and outgoing solar radiation at three-hour intervals. Cloudiness data are available from regular weather reports sent from Aboa.

3.1 Physical properties of snowpack

The physical properties of the snowpack in the study area are relatively well known through earlier investigations during austral summers (e.g. Isaksson and Karlén, 1994; Richardson-Näslund, 2004; Kanto, 2006; Rasmus, 2009; Ingvander et al., 2011). In the study area, the distance from the coast is more important factor controlling the variations in snow properties than the surface elevation and the properties vary between the ice shelf, coastal region and polar plateau (Kanto, 2006). On the ice shelf the mean snow density of the topmost metre is 394 ± 26 kg m^{-3} (± standard deviation, S.D.), in the coastal region 396 ± 30 kg m^{-3}, and on the plateau 367 ± 22 kg m^{-3}. The grain size of the topmost metre on the ice shelf is 2.0 ± 1.0 mm (± S.D.), in the coastal region 1.5 ± 0.7 mm and on the plateau 1.0 mm. The mean grain size in the annual layer varied between 1.5 and 1.8 mm and decreased exponentially with increasing distance from the ice edge by 18 %/100 km. The predominant grain shape is rounded (Kanto, 2006). Stephenson (1967) reported that the variation in the snow grain size with depth is most rapid in the topmost few centimetres. Depth hoar layers are usually found under the thin (1–2 mm), hard ice crust and are associated with a low complex permittivity (Kanto, 2006). These results probably also apply to winter snowpack, but measurements in winter have never been conducted.

3.2 Surface energy and mass balance

The surface energy balance in DML is strongly connected to the surface slope and hence to the strength of katabatic wind (Reijmer and Oerlemans, 2002). Only in vast and homogeneous areas the local surface energy budget governs the near surface climate. Otherwise the near surface climate controls the local surface energy balance. Generally the annual averaged energy balance is dominated by a negative radiative flux balanced mainly by the positive sensible heat flux (Reijmer and Oerlemans, 2002). The surface energy balance consists of five main components and can be written as:

$$Q_{SW} + Q_{LW} + Q_H + Q_{LE} + G = 0 \tag{3.1}$$

in which Q_{SW} and Q_{LW} are the net shortwave and net longwave radiative fluxes, respectively, and Q_H and Q_{LE} are the turbulent fluxes of sensible and latent heat, respectively. G is the subsurface energy flux including surface melt.

The heat flux from the snow cover can be estimated, using the temperature gradient in the top part of the snow cover:

$$k_t = \frac{\partial T}{\partial z}|_{z=0} = Q_n \tag{3.2}$$

where k_t is the thermal conductivity, T the temperature, z the depth and Q_n the energy balance at the surface. Here Q_n consists of four main components and can be expressed as:

$$Q_n = Q_{SW} + Q_{LW} + Q_H + Q_{LE} \tag{3.3}$$

Several surface energy balance investigations have been performed in western DML (e.g. Reijmer and Oerlemans, 2002; Van den Broeke et al., 2005, 2006). Reijmer and Oerlemans (2002) reported the annual average energy gain at the surface from the downward sensible heat flux varies between approximately 3 W m^{-2} and 25 W m^{-2}, with the highest values at the sites with the largest surface inclination and wind speeds. The annual average surface net radiation balance is negative (towards the air) ranging from about -2 W m^{-2} to about -28 W m^{-2} and largely balances the sensible heat flux. Maximum values of the net radiation balance can be linked to maxima in surface slope and wind speed. The average latent heat flux is generally small and negative ($\sim$ -1 W m^{-2}) indicating a slight net mass loss through sublimation. During the short Antarctic summer, the net radiation becomes slightly positive (towards the surface) (Van den Broeke et al., 2005). The daily cycle of the surface energy balance is driven by absorbed shortwave radiation. During the night, heat is re-supplied to the snow surface by the sensible heat flux, especially in the katabatic wind zone, and the sub-surface heat flux (Van den Broeke et al., 2006). The surface energy balance is strongly dependent on cloud cover.

The surface mass balance is partly connected to the surface energy budget. For instance, the katabatic wind blows when the near surface air is cooled as a result of a negative net radiation balance and the katabatic wind can erode snow from the surface (Reijmer and Oerlemans, 2002). The relationships between the spatial variations in snow accumulation and the katabatic outflow have been recognized long time ago, but are poorly understood (Gow and Rowland, 1965;

Melvod et al., 1998). The surface mass balance, *SMB*, consists of five main components and can be express as:

$$SMB = PR + SU_s + ME + ER_{ds} + SU_{ds} \tag{3.4}$$

in which PR is solid precipitation, SU_s surface sublimation/deposition, ME melt, ER_{ds} erosion/deposition due to divergence/convergence of the horizontal snowdrift transport and SU_{ds} sublimation of drifting-snow particles in a column extending from the surface to the top of the drifting-snow layer (Van den Broeke et al., 2004b). Components are defined as negative when they remove mass from the surface.

The spatial variations in snow accumulation are well known in western DML. The yearly snow accumulation has been studied through stake surveys, oxygen isotope measurements, firn cores and radar profiling, and sonic altimeters (e.g. Isaksson, 1992; Isaksson et al., 1996; Richardson et al., 1997; Van den Broeke et al., 2004b; Granberg et al., 2009; Boening et al., 2012). The mean annual snow accumulation on the ice shelf is 312 ± 28 mm w.e. (± S.D.), in the coastal region 215 ± 43 mm w.e., and on the plateau 92 ± 25 mm w.e. (Kanto, 2006). The accumulation decreases with elevation and distance from the coast (Reijmer and Oerlemans, 2002). On the polar plateau, the accumulation consists mainly of very small snow grains called 'diamond dust' which falls almost continuously from the sky (King and Turner, 1997). Net accumulation of snow on Basen is influenced by precipitation, snowdrift, sublimation, and summer melting.

AWSs were used in the heat and bass balance investigations. Institute for Marine and Atmospheric Research Utrecht (IMAU), the Netherlands, installed nine weather stations to western DML during the austral summer 1997–1998 (Reijmer and Oerlemans, 2002). Nearest AWSs to Basen are AWS 4 (34 m.a.s.l., dismantled Dec 2002) and 5 (365 m.a.s.l., operational). The AWS 4 was located on the ice shelf about 60 km from Basen towards northwest and the AWS 5 is located on the continental ice sheet 10 km from Basen towards the southeast. The AWS 4 and 5 have measured meteorological parameters including air temperature, relative humidity, wind speed and short- and longwave radiation since the austral summer of 1997 (Reijmer and Oerlemans, 2002). The net snow accumulation was measured using SR 50 acoustic sensor (Campbell Scientific Ltd., USA).

3.3 Blue ice areas

Several studies about the BIAs have been performed in western DML (e.g. Holmlund and Näslund, 1994; Bintanja et al., 1997; Bintanja, 1999; Keskitalo et al., 2013). The difference between the average surface heat balance over blue ice and snow surface is clear. Due to its lower albedo, blue ice absorbs solar energy approximately twice as much as snow. This causes the blue ice temperatures to be higher than the snow temperatures, which results in increased sublimation and a negative surface mass balance (Bintanja, 1999). Thermodynamics of the supraglacial lakes is governed by the summer radiation balance: penetration of solar radiation provides heat for subsurface melting of ice, and therefore the surface must be essentially snow-free. A supraglacial lake may have an ice cover, if longwave radiation and turbulent heat losses overcome absorption of solar heat

at the surface. The annual cycle of the surface energy balance shows that heating of the ice occurs mainly in early summer, whereas steady cooling takes place during the rest of the year (Bintanja et al., 1997)

The largest supraglacial lake located in the study area is lake Suvivesi at the southwestern side of Basen (Fig. 3.2). Lake Suvivesi extends 4 km out from Basen and its surface area is at maximum approximately 7 km^2. The lake forms and grows from patches, and therefore it is difficult to determine the evolution of the surface area. Lake Suvivesi is also used as a source of household water for Aboa station, and therefore practical experience of its formation is available since 1990. Supraglacial lakes are also known to form next to Plogen and Fossilryggen nunataks at distances of 25 km and 50 km, respectively, from south of Basen. At Basen and Plogen, the lakes are at the level of the surface of the neighbouring ice sheet, whereas at Fossilryggen the lake is in a 200-m deep hollow around one of the nunatak peaks, about 400 m.a.s.l. These supraglacial lakes are extremely low in biota (Keskitalo et al., 2013).

Supraglacial lakes are a common feature in the Greenland ice sheet, and there they are much more developed and have a major impact on the ice mass balance (Hoffman et al., 2011; Liang et al., 2012). Lake outflows may form moulins into the ice advecting heat into the ice sheet interior and reducing the sliding friction at the base of the ice sheet.

Figure 3.2: A photograph of lake Suvivesi taken from the top of Basen, 15 January 2005. A low moraine ridge is seen in the middle of the lake.

4. Methods

Following main methods were used when collecting data for this thesis in Finland (Bay of Bothnia and lake Kilpisjärvi) and in Antarctica (Table 4.1). Data from Finland was collected in spring 2008 and 2009. Data from Antarctica was collected during the field campaigns in austral summers 2004–2005, 2009–2010 and 2010–2011.

Table 4.1: *Summary of field measurements.*

Site	Snow pits	Automatic snow stations	Light transmission	Radiation balance	Ice core/ Lake studies
Finland	2008 & 2009	-	2008 & 2009	-	-
Antarctica	2009 & 2010	2009 & 2010	2009	2004 & 2010	2004 & 2010

4.1 Snow pits

Snow pits were dug to record temperature, layering, size and shape of snow grains, hardness, density, LWC, and salinity. In Antarctica, the physical characterization of snow stratigraphy was done at 5-cm or 10-cm vertical resolution and in Finland, at 5-cm vertical resolution.

The temperature profiles were measured, using a digital thermometer (EBRO TLC1598, Argus Realcold Ltd, Auckland, New Zealand) with resolution of 0.1 °C and an accuracy of ± 0.2 °C. The size and shape of the snow grains were determined, using an 8x magnifier and a millimetre-scale grid. The snow-type classification followed The International Classification for Seasonal Snow on the Ground issued by IACS (Fierz et al., 2009). Photographs were also taken to give visual confirmation of the shape and size of the snow grains. The reported snow grain size is the greatest diameter of a grain. Hardness was measured, using a hand test. The hand hardness test uses objects of decreasing areas and the index corresponds to the first object that can be gently pushed into the snow (fist = very soft, 4 fingers = soft, 1 finger = medium, pencil = hard and knife = very hard). The hand test is a relative and subjective measurement.

The snow density was measured directly, using a cylinder sampling kit with a volume of 0.25 dm^3 (diameter 5 cm), a metal box with volume of 1 dm^3 (5 cm x 13 cm x 15.4 cm (H x W x L)) and a Pesola spring balance with 5-g resolution (Pesola AG, Baar, Switzerland). The accuracy was estimated as ± 10 kg m^{-3}. The LWC was measured, using a snow fork manufactured by Toikka Oy, Finland. The snow fork is a resonator that can be pushed into the snow to determine the complex permittivity from the change in the resonance curve (Sihvola and Tiuri, 1986). The imaginary part of complex permittivity is predominantly dependent on the

LWC, while the real part is dependent on the density and the LWC (Sihvola and Tiuri, 1986). The imaginary part is negligible in dry snow. These dependencies allow the density and the LWC of snow to be estimated. The manufacturer has stated that the accuracy for the density is $\pm$ 5 kg m^{-3}, $\pm$ 0.3 % units for the LWC expressed as a percentage by volume, and the LWC measurement range is from 0 % to 10 %. The density data showed similar vertical profile structures but were biased down (values were smaller), compared with the direct measurements. Therefore, density values from the snow fork measurements were not used in the present study. For the LWC control we do not have independent data, apart from qualitative judgment when working in snow pits.

Salinity was measured only from the snow samples collected on the sea ice in the Bay of Bothnia, Baltic Sea. The salinity was measured from the meltwater of the collected snow samples using a handheld conductivity probe, which provides salinity of seawater solutions. This was done, because large amounts of solid salt crystals can affect the light transmittance (Perovich, 1998). The snow samples were melted in pre-cleaned airtight containers.

4.2 Automatic snow stations

The snow station provides a method for recording the temperature time series in the active surface layer. The temperature data can be used to calculate the heat flux of the snowpack and to determine the snow accumulation. Two snow stations were deployed for one year and the data collection was successful, lasting about 400 d (9 Dec 2009–21 Jan 2011). Snow station 1 was installed on the Riiser-Larsen Ice Shelf 40 km northwest of Aboa and snow station 2 was installed next to AWS 5 on the continental ice sheet 10 km southeast of Aboa. The snow stations were installed in open snowfields that were relatively flat and without any visible crevasses inside a 10-km radius to minimize the effects of the local topography on the snow accumulation. The goal was to find a site representative for a larger area (ice shelf or continental ice sheet) thus e.g. sloping surfaces near the grounding line should be avoided, because the snow accumulation may be completely different and not representative for the larger area. In this way the data could be used in snow cover and climate modeling studies. At each site a 1.5-m-deep snow pit was dug during installation and retrieval to record the physical properties of the snowpack.

Here is presented a short summary about the technical specifications of the snow station. More detailed information can be found in Omega (1992) and Paper III. Both snow stations are comprised of 20-mm-diameter rigid plastic tubing, 4.5 m long, having inside a 20-pair cable, about 8 m long. The cable was longer than the plastic tubing to enable it to reach the logger box. To minimize radiation errors, the plastic tubing and the cover of 20-pair cable were manufactured from white high-reflectance plastic. The distance between the sensors attached to the 20-pair cable varied from 8 cm to 52 cm. The thermistor has a resistance that varies inversely with the temperature: if the temperature increases, the resistance of the thermistor decreases. The cable with the thermistors was connected to a CR1000 data logger (Campbell Scientific Ltd., USA), which is resistant to low-temperature-conditions (Vehviläinen, 2010). The logger and 12-V DC lead-acid batteries were placed in insulated boxes that could withstand the weight of the

snowpack.

A Kovacs MARK II coring system was used to drill a 4-m-deep vertical hole. The sensor rod was inserted into the hole and the sensors were turned to face the wall of the hole to connect with the undisturbed snowpack. After that the hole was filled with snow and bamboo poles were used to pack the snow tightly so that the temperature sensors would have a good connection with the snowpack. Flagged bamboo poles, 1.5 m long, were used to facilitate finding the stations one year later. The installation procedure took less than 15 minutes. Thus we estimate that the installation did not cause a significant disturbance to the temperature profile. In situ tests showed that the snow density did not change significantly when bamboo poles were used to pack the snow tightly.

4.3 Light transmission

Spectral measurements of solar radiation were performed above and inside the snowpack, using a spectroradiometer (model: NT58-657) manufactured by Edmund Optics Inc. Barrington, NJ, USA. The wavelength range was from 380 nm to 1050 nm, the spectral resolution was 1.5 nm, and measurement sensitivity was 0.002 μW cm^{-2} nm^{-1}. The spectroradiometer had a fixed quartz cosine receptor and was calibrated to measure absolute spectral irradiance of the light sources. The broadest measurement band used in data analyses was 400–900 nm due to the high noise level outside this band.

A snow pit with horizontal tunnel was dug with the aid of square shaped metal container with open ends. A spirit level was used to confirm that the tunnel was horizontal. The spectroradiometer was then placed at the end of the tunnel. The tunnel was closed with a piece of black foam plastic before the measurements, and a cardboard plate was used to prevent leakage from the open wall of the snow pit. In Antarctica, we could also use the snow block that was cut to make the tunnel. The tunnel length was at least twice the snow-cover thickness, making wall corrections unnecessary (Bohren and Barkstrom, 1974). The measuring sequence was the following: incident - transmitted - incident - transmitted - incident irradiance, and was applied for every depth. This was done because we had only one spectroradiometer in use; it required about 1-min to do the full sequence. Average values for the incoming and transmitted spectral irradiance were calculated and these averages were used to calculate the transmittance and extinction coefficient. Dark spectra (electrical noise) were recorded in the field by capping the fixed quartz cosine receptor.

Photosynthetically active radiation (PAR) was recorded in the Antarctic snowpack and in supraglacial lakes, using small cylinder-shaped (115 mm length, 18 mm diameter) scalar quantum irradiance sensors (model: MDS-L). The PAR sensors were manufactured by JFE Advantech Co. Ltd, Kobe, Japan. They were calibrated by the manufacturer for hemispheric scalar quantum PAR irradiance (spectral band 400–700 nm) and recorded the incoming quantum irradiance at 10-min intervals. Sensors are equipped with internal memory. In snow the PAR was measured from the surface down to depth of 30 cm. At the lake sites in BIAs, the sensors were lowered through narrow drill holes into the lake and anchored to the top surface with bamboo crosses.

4.4 Radiation balance

The net radiation and the spectrally integrated incoming and outgoing solar radiation at the surface were measured in lake Suvivesi and on Basen nunatak next to Aboa research station. The recording interval was 10 minutes. The net radiation was measured using a Kipp & Zonen (Delft, The Netherlands) NR Lite net radiometer (spectral range 0.2–100 μm) installed just above the ice/snow surface. The instrument was mounted on the end of a pole, which was clamped onto a tripod with sensor head about 1 m above the ground. The downwelling and upwelling solar planar irradiances just above the surface were measured with a Middleton (Carter-Scott Manufacturing Pty. Ltd. Melbourne, Australia) EP-16 pyrano-albedometer system (spectral range 300–3000 nm). The instrument is a modified thermopile pyranometer with an additional inverted sensor assembly. The instrument was mounted on a tripod in the same way as the net radiometer, and the two tripods were deployed close to each other.

The Aboa weather station (497 m.a.s.l.) located on Basen provided incoming and outgoing solar radiation at three-hour intervals. Gaps in the data were filled by interpolation. The AWS 5 (365 m.a.s.l.) measured the incoming and outgoing solar radiation (1-h interval), using the CNR1 net radiometer manufactured by Kipp & Zonen (spectral ranges 305–2800 nm and 5000–50000 nm).

4.5 Ice cores

Three sites were chosen for the investigations of the supraglacial lakes. The primary site was lake Suvivesi at the southwestern side of Basen; two additional sites located at Plogen and Fossilryggen nunataks. At Basen and Plogen, the lakes were at the level of the surface of the neighbouring ice sheet, whereas at Fossilryggen the lake was in a 200-m deep hollow around one of the nunatak peaks, about 400 m.a.s.l..

The basic structure of all three lakes was mapped by drilling with a Kovacs Ice Auger drill (diameter 55 mm) for the layers of solid ice, water and slush. Cross-sectional profiles of lake Suvivesi were drilled several times in 2004–2005 and 2010–2011 to obtain the history of evolution. Plogen lake site was visited once in 2004–2005 and twice in 2010–2011. The lake in the hollow in Fossilryggen was visited once (31 Dec 2004). A Kovacs MARK II coring system (diameter 90 mm) was used to drill from the surface down to 1–2 m beneath the lake bottom into the solid ice sheet. The ice cores provide information about the lake history, crystal structure of ice, and impurities. Temperature profiles of ice were determined from the cores at the sites.

The crystal structure of the ice cores was investigated by making so-called thin sections. The technique relies on the fact that ice crystals are able to alter the polarization of light. Approximately a 1-cm-thick slab of ice was cut using a band saw. The ice slab was placed on a glass plate and grounded down to a thickness of about 1 mm using a hand plane. The thin section was then placed between two crossed polarization filters. The ice crystals alter the polarization, each crystal will take on a color that depends on the orientation of the crystal thus the size and orientation of the crystals can be measured.

5. Results

This chapter is divided into subsections by the study topics. First are presented results from light transmission measurements. Then are presented results from supraglacial lake studies followed by surface mass balance results. Finally results from heat flux and power spectra calculations are presented.

Light transmission in snowpack was monitored using spectroradiometer and PAR-sensors in three locations; on the ice of Lake Kilpisjärvi, Northern Finland, on the sea ice in the Bay of Bothnia, Baltic Sea, and on the continental ice sheet in Antarctica (Papers I and IV). In Antarctica, light transmission in the supraglacial lake was also examined. In addition to the light measurements, the physical properties of snow were measured. Here, diffuse light condition means that there were clouds in the sky so that the Sun was no longer visible behind them. Direct light condition means that the Sun's direction was cloudless, so that direct radiation was received when the measurements were performed.

Light transmission in Finland

The main goal with light transmission measurements in Finland in spring 2008 and 2009 was to develop a suitable light transmission measurement technique for a "box-like" spectroradiometer that do not have a fiberoptic probe (Paper I). After the extensive test campaign, where we studied e.g. effects of the open wall, the snow/foam plastic filled tunnel and tilted spectoradiometer on the irradiances measured in the snowpack, the suitable measurement technique was developed.

Measurements in Kilpisjärvi and in the Bay of Bothnia revealed large variations in transmittance and extinction coefficient depending on the physical properties of snowpack (snow density, grain size and type) and light conditions (Paper I). The transmittance varied from < 1 % (0–12-cm layer) to 80 % (0–4-cm layer), and the extinction coefficient was between 0.03 cm^{-1} (4–8-cm layer) and 0.8 cm^{-1} (0–4-cm layer). There were clear differences in the transmittance profiles between diffuse and direct light conditions, especially at 4 cm, because under direct light conditions the radiation field is not yet totally diffuse at this depth. Therefore the calculated extinction coefficients of the 0–4-cm layer must be interpreted carefully. At greater depths (4–8-cm and 8–12-cm layers), the extinction coefficient profiles were quite similar between direct and diffuse light conditions indicating that the radiation field is diffuse at these depths. The extinction coefficients were almost twice as high in the Bay of Bothnia as in Kilpisjarvi and this can be probably be explained by differences in density and predominant grain types.

The grain size and shape were quite similar within the lake site and sea site locations, but varied widely between the locations. In the Bay of Bothnia, highly broken particles predominated, but in Kilpisjärvi the rounded mixed form predominated. The density of the snow varied between 140 and 480 kg m^{-3} and

the highest density value was measured in Kilpisjärvi. The snow densities were generally slightly higher in Kilpisjärvi than in the Bay of Bothnia. The salinity levels were low in the upper part of the snowpack in Bay of Bothnia and thus presumably did not affect the irradiance values.

Light transmission in Antarctica

In Antarctica (Paper IV), light transmission measurements were conducted between 19 Dec 2009 and 9 Jan 2010 on the continental ice sheet. The short integration times caused noise in the 380–420-nm band and in the wavelengths higher than 900 nm. Therefore the lowest and highest reliable wavelengths that we could use in our measurements were 400 nm and 900 nm, respectively.

The transmittance was measured for two layers: 0–10-cm and 10–20-cm layer. Transmittance varied between locations depending on the predominant grain shape and light conditions. The effects of the surface and depth hoar layers were clearly seen. Also the elevation of the Sun affected the transmittance. The transmittance was < 1 % through the upper 20 cm and up to 27 % through the upper 10 cm. The lowest values were recorded in the near-infrared band (750–900-nm).vIn the near-infrared band the transmittance decreased to almost zero.

The diffuse extinction coefficient was estimated for two layers: 0–10-cm and 10–20-cm layer. The mean spectral diffuse extinction coefficient in the 0–10-cm layer varied between 0.13 and 0.5 cm^{-1}. The largest variation in density occurred in the upper layer (0–5 cm) and the variation in snow grain size with depth was most rapid in the topmost few centimeters. Also the 0–10-cm depth range contains the nondiffuse zone, therefore the results for the 0–10-cm layer must be interpreted carefully. Diffuse extinction coefficient in the 10–20-cm layer varied only slightly between locations (Fig. 5.1). Only the FR137 location stood out due to the 5-cm thick depth hoar layer (the predominant crystal size was 2 mm). The mean spectral diffuse extinction coefficient varied between 0.04 and 0.31 cm^{-1} (10–20-cm layer). The largest values were recorded in the near-infrared band and there was no sharp distinct minimum, but rather a minimum band at 400 nm. The mean diffuse extinction coefficient at 400 nm was 0.04 cm^{-1} (snow density 370 kg m^{-3}; grain size: 1 mm; shape: rounded). The theoretically calculated average depth, using the spectral extinction coefficients of the 0–10-cm and 10–20-cm layers where broadband irradiance (400–700-nm band) was 1 % of the downwelling irradiance at the surface, was 50 cm.

The diffuse extinction coefficient from the PAR sensors for the 10–30-cm snow layer was 0.082 cm^{-1} (snow density 375 kg m^{-3}; grain size: 2 mm; shape: rounded) and 50–70 cm^{-1} for slushy body (0–60-cm layer) of the lake Suvivesi (Paper II and IV). Using the PAR diffuse extinction coefficient (10–30-cm snow layer) and measured light quanta values from the PAR sensor measurements in the snowpack, we obtain 60 cm for the 1 % depth. In aquatic ecology, the euphotic depth is usually referred to as the depth at which the downwelling irradiance is 1 % of the downwelling irradiance just below the surface. The euphotic depth is the depth that is exposed to sufficient sunlight for primary production. The obtained 60 cm can be taken as a lower boundary, since it is likely that under cold conditions primary production can occur with fewer photons than under normal oceanic surface-layer conditions.

The snow density in the upper part of the Antarctic snowpack (0–55-cm layer) varied between 300 and 440 kg m^{-3}. The mean density increased with depth and the variation decreased slightly. The large rounded snow particles predominated and the predominant grain size was 1 mm in every snow pit, but at one location there was a a 4-cm-thick surface hoar layer and at another location a 5-cm-thick depth hoar layer. The LWC varied from 0.53 % to 2 % which also corresponded to qualitative judgment in the field. The average LWC from the snow pits varied between 0.77 % and 1.36 %.

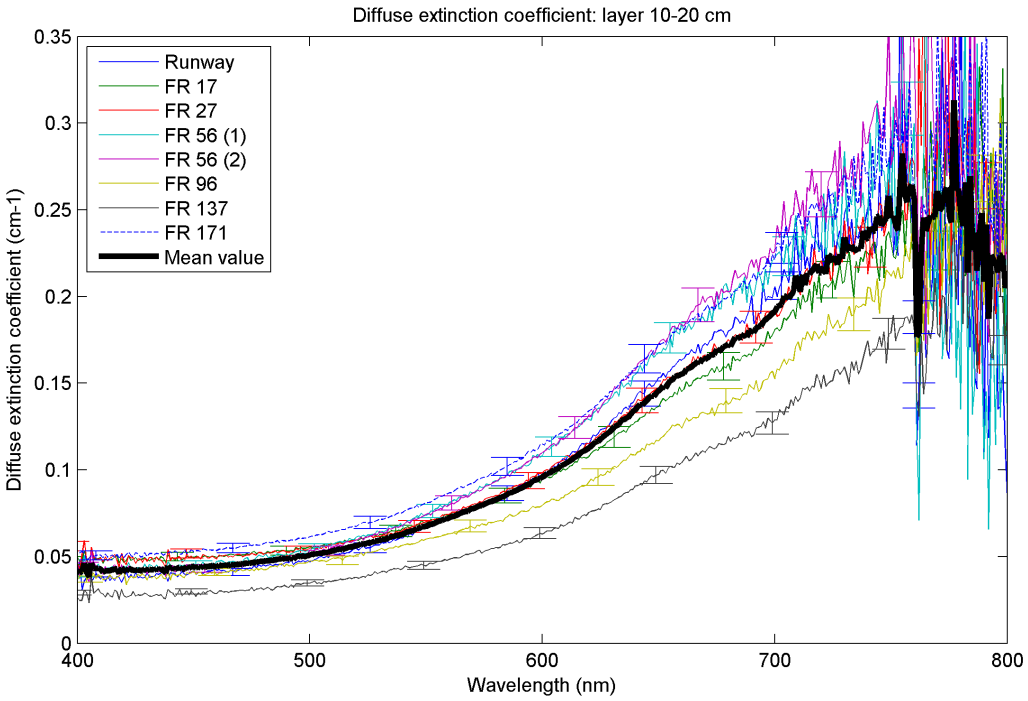

Figure 5.1: Diffuse extinction coefficient for 10-20-cm snow layer from each snow pit measured in western DML.

Supraglacial lake studies

Seasonal evolution of three supraglacial lakes was examined in austral summers 2004–2005 and 2010–2011 (Paper II). The vertical profile evolution of lake Suvivesi in summer 2004–2005 and 2010–2011 is shown in Figure 5.2. Based on these two seasons, the evolution of the central area of lake Suvivesi (primary site) can be summarized as follows. The lake starts to form in the solid ice sheet in the beginning of December. At about the 10th of December there is enough liquid water for water supply to Aboa station (the timing has a very small inter-annual variability). At the initial stage the lake appears patchy in the horizontal plane. In January there is a 0–10-cm thick ice cover on top and the lake body extends down to about 200-cm depth consisting of two layers. The main, upper layer is mostly liquid water and extends down to the depth of 0.5–1 m. The lower layer is a soft bottom layer and contains slush and hard ice. It contains at least one slush sub-layer and one hard ice sub-layer and the deepest part is an 'under-lake slush pocket', at the bottom of which there are gravel and soil sediments. The source of these sediment particles is most probably the neighbouring nunatak.

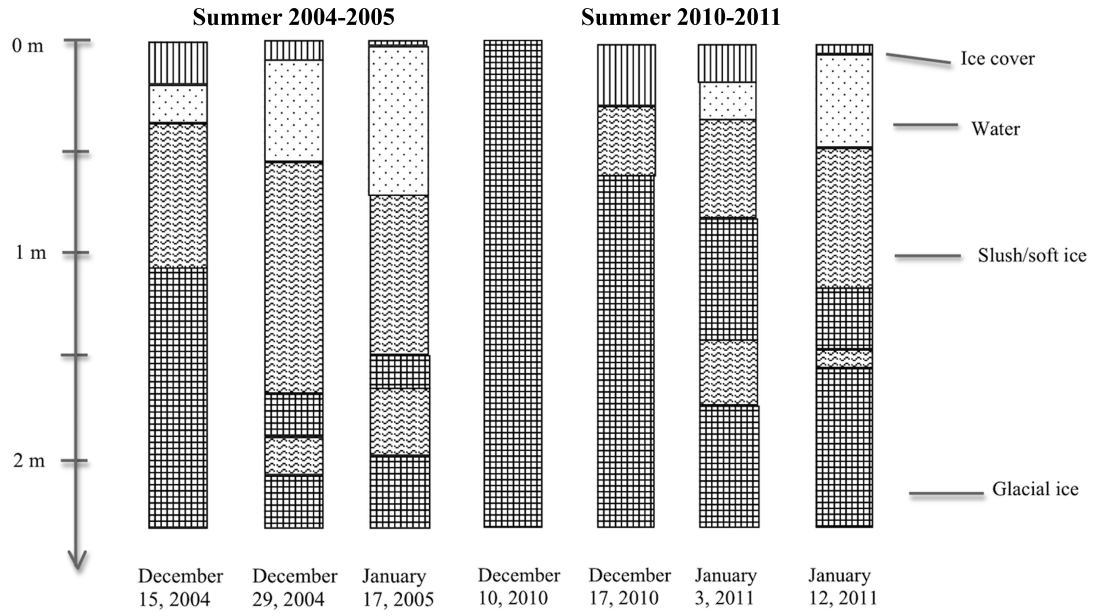

Figure 5.2: The vertical profile of lake Suvivesi in December 2004–January 2005, and December 2010–January 2011.

After the summer warm peak in atmospheric conditions in mid-January, the surface ice layer starts to strengthen, but the main body of the lake continues to develop due to the positive radiation balance. We have no observation beyond February 1st, and it is not exactly known when the lake shrinking by freezing begins. Based on experience of lake ice growth in general, this can be estimated. In the closing period of the lake, the growth of ice is expected to be 1–2 cm per day. With this rate, the lake would be completely frozen by April - May.

The growth of ice in the closing season (surface radiation balance < 0) was calculated using the Zubov's law (Zubov, 1945, see also Leppäranta, 2009). When the air temperature T_a is below zero in the lake closure season, the ice growth is obtained from Zubov's law:

$$h = \sqrt{aS + b^2} - b \tag{5.1}$$

where S is the sum of freezing-degree-days, and $a \approx 11$ cm^2 day^{-1} °C^{-1} and $b \approx 10$ cm are the model parameters. In exact terms, $a = 2k_t/(\rho L)$, where k_t is thermal conductivity, ρ ice density and L latent heat of freezing, and $b = k_t/K_a$, where K_a is ice-air heat exchange coefficient when taking the heat transfer as $K_a(T_0 - T_a)$. Thus a depends on the physical properties of ice and varies very little, while b is a more free parameter as it is connected to the heat transfer from ice surface to atmosphere.

In snow-free conditions, as here, K_a is roughly proportional to the mean wind speed, and when also $\sqrt{aS} \gg b$, the annual ice accumulation is not very sensitive to b: $h \approx \sqrt{aS} - b$. With ten months close-up season and mean air temperature of -15 °C (Kärkäs, 2004), we have $S = 4500$ °C·day and thus $h = 2.13$ m. In addition, the lake also loses heat to the deeper ice sheet. Taking the temperature gradient as 1 °C m^{-1} beneath the lake, the heat loss would be 2 W m^{-2}. In ten months this corresponds to 18 cm ice growth. Ice thickness is approximately $h \approx \sqrt{aT_m t}$, where T_m mean air temperature (°C) and t is time, and hence (apart from thin ice cover in temperate climate zone) it is not very sensitive to

temperature variations. In the present case, ± 3 °C overall change in the air temperature would change the ice thickness only ± 20 cm.

In summary, the inferred age of the lake is 4–6 months, 1–2 months for growth and 3–4 months for close-up. Observations from lakes at Plogen and Fossilryggen showed similar evolution but the exact timing depended on the location. No deep-water layer was found in the beginning of summer when drilling the first ice core samples and therefore we can say that the present study lakes freeze completely during winter.

The surface ice layer exists because the surface energy balance in this region is negative. Large amount of the incoming solar radiation penetrates into the ice (and liquid water beneath), and the surface absorption does not compensate for the thermal radiation loss. The thin ice cover corresponds to the 'cold skin phenomenon' observed in lower latitude lake and sea surfaces in daytime calm summer conditions (e.g. Fedorov and Ginzburg, 1992).

Water-pumping experiments (Paper II) were made to examine the hydraulic conductivity, K, of the lake Suvivesi and the Dupuit well equation (e.g. Raghunath, 2007) was used to calculate the hydraulic conductivity:

$$2\pi r_0 DK\frac{\partial \xi}{\partial r} = V \tag{5.2}$$

where r_0 is the radius of the pump hole, D the depth of the pump hole, ξ the water surface level at the site, r distance from the centre of the hole, and V the discharge rate in pumping. The water-pumping experiment site was in the boundary region of the lake where the surface ice thickness was 15–30 cm with additional support from the underlying slush. The site was changed three times during the field season because of the lake evolution. At the first site (14–17 Dec), K increased from 0.25 to 0.80 cm s^{-1}; at the second site (18–27 Dec), K varied between 1.5 and 2.0 cm s^{-1} during the first week but suddenly increased to 8.0 cm s^{-1} on the 27 Dec; at the third site (28 Dec - 27 Jan), initial K was 0.8 cm s^{-1}, increased to 2.0–6.2 cm s^{-1} in 4–14 Jan, and in 18–27 Jan was as high as 20–30 cm s^{-1}.

A Darcy-type experiment was also conducted to estimate the hydraulic conductivity of closely packed slush which served as a good reference to the water-pumping experiment. A pipe, 1-m-long and diameter of 20 cm, was filled with slush, tilted, and then water was let to flow through. The hydraulic conductivity was obtained from the time water flew through the pipe, resulting in $K = 6.3$ cm s^{-1}. Water storages with hydraulic conductivities greater than 0.01 cm s^{-1} are classified as good in groundwater hydrology, and conductivities less than 1 cm s^{-1} are typical for gravel. The hydraulic conductivity is important to know when modeling the circulation in supraglacial lakes and it serves also as an index for the internal structure of the lake.

Lake Suvivesi water was very clean, classified as an ultra-oligotrophic lake (Paper II). Electric conductivity was 1–10 μS cm^{-1} (25 °C) and pH ranged between 6 and 8. Sediment particles consisted of soil and gravel. The source of impurities was the neighbouring nunataks, from where they were transported by air. No systematic spatial variations were observed. Closer to the nunatak the conductivity and pH were similar as in the central area. Electric conductivity showed decreasing trend during summer, and pH decreased in the first half of summer and increased in the second half. Similar levels and temporal variations

were observed in other measurement sites as well. In summer 2010–2011 the total nitrogen and phosphorus were 60–100 mg m^{-3} and 1–2 mg m^{-1}, respectively, close to the levels recorded in the surface snow layer (Keskitalo et al., 2013). Thus the transport of surface material from the nunatak bare ground to lake Suvivesi was by winds rather than by hydraulic systems.

Lake Päijanne, located in central Finland, is the second largest lake and considered as a clean lake in Finland. Electric conductivity is 78 μS cm^{-1} (25 °C) and pH is 7. Total nitrogen and phosphorus levels are 487 mg m^{-3} and 4 mg m^{-3}, respectively (Leppäranta et al., 2003). All the levels, except pH, in lake Päijanne are clearly higher than in lake Suvivesi. The pH level is practically the same in both lakes.

Surface mass balance

The annual net snow accumulation 600 m away from snow station 1 was 79 cm (286 mm w.e.) (Paper III). It was measured from a snow pit dug 600 m away from the snow station 1 due the safety reasons (small crevasses visible). Snow station 1 was installed during poor weather conditions on the border of the continental ice sheet and the ice shelf. Therefore we did not notice that the site located on a gentle slope on the lee side relative to the prevailing wind direction in the area and this caused the unexpectedly high annual snow accumulation at snow station 1 that was over 150 cm. The annual net snow accumulation at snow station 2 measured from the bamboo poles, resulted in an 86-cm snow layer (345 mm w.e.). Based on the annual snow layer data, the compaction rate for snow station 2 location (continental ice sheet) was 0.0201 ± 0.02 y^{-1} and 600 m away from snow station 1 (ice shelf) the compaction rate was 0.675 ± 0.02 y^{-1}. The high compaction rate on ice shelf was due to the exceptionally low snow density value measured at the surface. The local variations in the surface density had a greater influence on the compaction rate than the accuracy based on the error margins of the density measurements.

The mass and heat balance investigations of snow patches (485 m.a.s.l.) in Basen nunatak revealed that much more snow was lost in summer 2010–2011 than in 2004–2005 (Paper V). Snow thickness decreased along the snow line on average by 5 mm d^{-1} (2 mm d^{-1} w.e.), and up to half of it was due to metamorphic compression of the snow cover and the rest is loss of mass by sublimation.

The snow pit profiles showed that snow melting did not become strong enough to initiate runoff, rather a small amount of moist snow was observed just beneath the surface. In the warmest summer peak the LWC was below 1 %. Later this meltwater refroze, resulting in melt-freeze metamorphosis within the snow pack. Thus runoff was very small if anything in the snow line, and it was evident that sublimation caused most of the loss of snow. However, close to boundaries of snow patches, where the snow cover was thin, the presence of melt water was noted. A plausible reason is that sunlight penetrates through thin snow, warms the soil surface underneath, and then snow can start to melt from the bottom. The snow-free soil was moist down to half-meter depth, the sources of water being the snow patches and the ice in the frozen ground. In the study area no liquid water ponds or pools were seen.

In 2004–2005 the rate of decrease of snow thickness was 4 mm d^{-1} w.e. and in 2010–2011 it was 6.3 mm d^{-1} w.e. A possible reason is that the thinner snow cover

decays a little faster, since solar heating of the ground can initiate snowmelt at the bottom of the snow cover. This feedback could be strengthened by mechanical erosion at the surface. In the course of summer 2010–2011, deep-sliced surface roughness structures were formed in the snow line area (Fig. 5.3). The slices were tilted and oriented toward north-northeast sector and evidently formed by the solar radiation. The slices become deeper in January, and snow thickness at the stakes was no more so well defined. Collapsing slices caused sudden drops in the thickness of snow. This thermo-mechanical erosion fastened the decay of snow. The bottom of the slices could reach bare ground even when the snow thickness was still 20–30 cm. Lateral decay (retreating of the edge) (sublimation and melting) erodes normal snow patches by 10 cm d^{-1}. The sublimation rate at the continental ice sheet (365 m.a.s.l.) in December 2010 was 0.64 mm d^{-1} w.e. (Paper III).

Figure 5.3: Sliced surface roughness of the main snow patch. Left: slices start to form (white-yellow marks in the meter stick are each 10 cm long). Right: in thin snow the slices have penetrated into the soil surface.

Heat flux and power spectra

For the heat flux and power spectra calculations, a temperature record at depth of *c.* 54 cm was constructed from the temperature records of seven sensors of snow station 2. The interval between the sensors and the rate of snow accumulation determined which depth was used for the temperature record.

The heat flux from the snow cover was estimated using equations 3.2 and 3.3 (Paper III). The turbulent fluxes of sensible and latent heat were calculated using bulk formulas. Negative values represent heat loss from the snowpack to the atmosphere and space. The temperature gradient between the snow surface and the depth of 54 cm was evaluated from the temperature data of snow station 2 to represent the heat flux across the upper part of the snowpack (Fig. 5.4). We observed an annual cycle in the flux direction that was quite faint. Most of the time the flux is negative, but in the summer months it becomes positive. Heat flux time series above the snow surface was also calculated using the data from AWS 5, but there is no clear annual cycle seen in the flux direction. The

uncertainties in the shortwave and longwave radiative fluxes and in the relative humidity caused some error to the estimated heat flux from the data of AWS 5.

There can be a special situation when the turbulent fluxes and the net longwave radiation are zero and the positive flux is caused by the solar radiation. Thus the positive flux is transfer of the solar radiation to the snow pack, not heat flux from the near-surface air. We used the temperature gradient between the snow surface and the depth of 54 cm to evaluate the heat flux in the upper part of the snowpack. Most of the solar radiation is absorbed during the first 10 cm and at the depth of 54 cm amount of the solar radiation is very small (∼1 %). Therefore we estimate that the error caused by the solar radiation is very minor.

In paper III we mentioned that negative values represent heat loss from snowpack to the atmosphere, but this is incorrect. In cloudless winter situations, the negative flux can be caused completely by negative net longwave radiation balance and part of the longwave radiation escapes to space. The simultaneous turbulent heat flux is typically from air to snow.

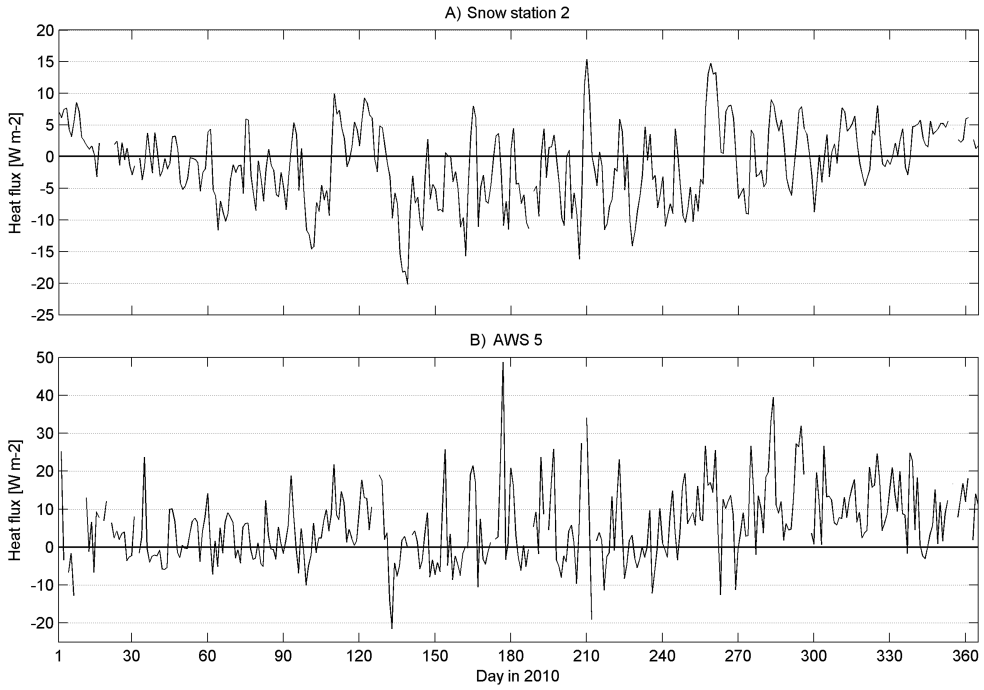

Figure 5.4: A) Heat flux time series estimated from the temperature data of snow station 2. Negative values represent heat loss from the snowpack to the atmosphere/space. B) Heat flux time series estimated from the data of AWS 5. Negative values represent heat loss from the snowpack to the atmosphere/space.

The power spectra calculations help us to identify the different snow temperature cycles that occur annually in the study area (Paper III). The power spectra of the snow temperature at a depth of 54 cm at snow station 2 revealed three distinct cycles. The shortest cycle was an one-day cycle caused by the daily cycle of the sun and thus it was only seen during the summer months (Fig. 5.5). A synoptic timescale (∼10 days) cycle and a long cycle, 60–120 days, were also seen. The two later cycles were visible throughout the entire year. The changes in the season are probably reason for the longest cycle. The present cycles can be used as a reference to the future measurements.

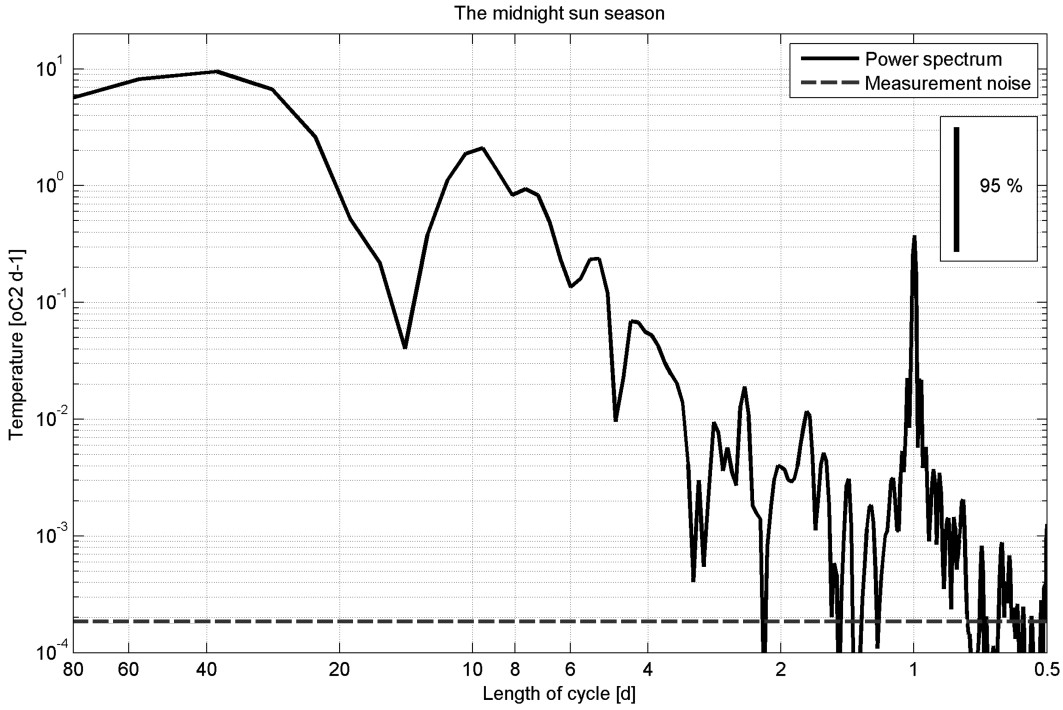

Figure 5.5: Power spectrum of the snow temperature at the depth of 54 cm for the midnight Sun season, estimated from the records of snow station 2.

6. Summary and final remarks

The present study focused on the active 10-m surface layer in western Dronning Maud Land, Antarctica. The data was collected during the FINNARP expeditions in the austral summers 2004–2005, 2009–2010 and 2010–2011. Additionally, two snow stations were installed in December 2009 for one year to acquire information about the annual snow heat and mass balance. Measurements were conducted to study the possible annual cycles in the upper part of a snowpack and in the blue ice areas - and clear cycles were found. Measurements in Finland before the Antarctica expeditions helped us to develop suitable measurement techniques which could be used in Antarctica and to test instruments in cold conditions.

Maybe the most challenging issue in conducting measurements in Antarctica is to get the instruments working properly throughout the whole field campaign or even over the winter season, e.g. snow station. The weather conditions are extremely harsh and cause high strain on the measuring equipment. The wind speeds can rise up to hurricane scale and the temperatures can change very fast due to the katabatic winds - and drop down to -40 °C for a long time. There is also limited capacity for fixing instruments. If an instrument breaks down and cannot be repaired, it is impossible to get a new one during the same field campaign. The weather conditions combined with isolated location also limit the possibility to conduct field measurements. During the storms, it is too dangerous to conduct measurements outside and the weather can remain bad for several days limiting the time on the field. Safety procedures must be taken into consideration when planning and conducting measurements in Antarctica.

The methods and instruments that we used were quite simple and practical, and proved to be reliable. An earlier snow station experiment, which was partly a failure, since the longest temperature record extended only six months (Granberg et al., 2009), provided us with important information about the technical requirements of snow stations. Based on this information we built an improved sensor system that proved to be very reliable. Both snow stations were fully operational after 400 days and had stored data continuously without any interruptions. The practical methods to study the evolution of the supraglacial lake are ice core samples, water-pumping experiments and light transmission measurements. All our instruments functioned without any major problems and we managed to gather valuable information about what is required to conduct measurements successfully at an isolated location in harsh conditions.

Light transmission measurements in Kilpisjärvi and in the Bay of Bothnia helped us to develop a practical method of measuring light transmission in a snowpack. The method is suitable for spectroradiometers that do not have a fiberoptic probe that could be inserted into the snowpack horizontally or vertically. In Antarctica this method is useful because of the hardness of the snow-

pack. At some places the surface layer is so hard, that even heavy track vehicles do not break the surface layer - but leave just minor marks on the snow surface. Thus it is easy to dig a horizontal tunnel without substantially disturbing the snowpack.

In Finland, the diffuse extinction coefficient varied greatly between the locations, but the diffuse extinction coefficient measured on the continental ice sheet in Antarctica showed only small variations between locations. Only one location stood out due to the different grain type. Based on the light transmission measurements conducted in Finland the Arctic snowpack is very heterogeneous compared to the snowpack in western Dronning Maud Land, Antarctica. We can also use the light transmission measurements to analyse differences between the Arctic and the Antarctic snowpack and the values presented here can be used as a reference to the future measurements at the same locations.

We reported that the mean diffuse extinction coefficient was 0.04 cm^{-1} at 400 nm. Beine et al. (2006) reported a value of 0.083 cm^{-1} at 400 nm in the surface layer (Browning Pass, Terra Nova Bay, Antarctica) and France et al. (2011) reported a value of 0.1 cm^{-1} at 400 nm (Dome C, Antarctica). The differences in the extinction coefficients could be explained by the differences measured in snow density, grain size, and shape. The stratigraphy of the snowpack must be described as accurately as possible to obtain reliable extinction coefficient values for certain types of snow. It is especially important to accurately measure the grain size and shape and LWC, because these parameters have a significant impact on the extinction coefficient. The diffuse extinction coefficient values presented here cannot be generalized over different areas in Antarctica unless the stratigraphy of the snowpack is similar among the locations.

In Antarctica, the light measurements were conducted during three weeks in the summer season and we did not notice any temporal effect in the measured irradiance values. The LWC varied slightly between locations, but there was no indication of a temporal effect on the amount of liquid water in the snowpack and snow temperatures stayed also clearly below 0 °C. The reason is most likely the locations of the measurement sites and the short period of time when the measurements were conducted. All measurements were conducted on the continental ice sheet where the effect of the summer season is smaller compared to the ice shelf. On the ice shelf the effect of summer season is clearly visible: the high LWC is the reason for the thick refrozen layers. Therefore measurements from a longer period of time are needed to observe the possible effects of the summer season on the physical properties of snowpack and thus to the light transmission.

The present soot level is unknown in the snowpack of the study area. Even a small amount of soot has a clear effect to the light transmission by absorbing light and shifting the absorption minimum (pure snow: 390 nm) to longer wavelengths (Warren et al., 2006). We recorded the minimum band at 400 nm, but it was difficult to determine if this really was the minimum band due to the effect of the noise. We do not believe that the research stations in the study area would cause enough pollution to affect the transmission of light in the snowpack, thus the snow is as pure as or even purer in our study area than at the location where Warren et al. (2006) conducted their measurements. In the future soot level in the snowpack might increase if the wind patterns change and more soot is transported from the lower latitudes. Therefore the present soot level should be measured to get a reference level for the future light transmission measurements.

The snow compaction rate was higher on the ice shelf (0.675 ± 0.02 y^{-1}) than on the continental ice sheet (0.0201 ± 0.02 y^{-1}) due to the exceptionally low surface density value, but the density evolution on the ice shelf can be a thermal-mechanical process due to the warmer weather and this process can cause very high compaction rates on the ice shelf, especially if the summer seasons become longer. The possibility of a higher compaction rate on the ice shelf than on the continental ice sheet must be taken into account when interpreting remote sensing data and producing surface mass balance models.

Analyses of the lake physics showed that the depth of supraglacial lakes scales with the light extinction coefficient, and the volume of liquid water scales with the length of summer and solar heating. The ice thickness in the present case was not very sensitive to temperature variations. In this study region, the liquid water layer thickness may reach 1.5 m, and winter freezing can, in theory, exceed the depth of 2 m. Thus the supraglacial lakes in the study region are seasonal. A small change in both summer length and summer radiation balance would transform the supraglacial lakes from seasonal to perennial. Therefore it is crucial to follow the energy flux over the BIA and the length of the summer seasons. If the lake would change to perennial permanently, although observing it might be difficult, this could be interpret as an indicator that the present local climate conditions have changed.

The major question with the supraglacial lakes is what happens during the close-up season. We know when and how the supraglacial lake forms, but at this moment there are no in-situ measurements conducted in austral autumn. All the field measurements have been conducted during the summer seasons. Thus we do not have exact information when and how fast the supraglacial lakes freeze up.

The supraglacial lake measurements revealed only very small interannual variability in the seasonal lake structure, but the mass balance studies of snow patches in Basen nunatak showed clear variability between two summer seasons; the later summer being clearly warmer than the first summer. The snow patches are more sensitive to the changes in the weather conditions and to the unusual weather conditions, e.g. precipitation of liquid water, than BIAs. Long time series are needed to relate changes in the snow patches to possible changes in the local climate conditions.

The present temperature cycles in the continental snowpack can be used as a reference to the future measurements. Snow surface layer temperature data from snow station provides an independent system for mapping the net surface heat balance and guides the coupling between ice sheet thermodynamics and atmospheric weather conditions.

References

Baker, J. M., K. J. Davis, G. C. Liknes. 1999. Surface energy balance and boundary layer development during snowmelt. *Journal of Geophysical Research*, **104**(D16), 19611–19621.

Beaglehole, D., R. Ramanathan and J. Rumberg. 1998. The UV to IR transmittance of Antarctic snow. *Journal of Geophysical Research*, **103**(D8), 8849–8857.

Beine, H. J., A. Amoroso, F. Domine, M. D. King, M. Nardino, A. Ianniello, and J. L. France. 2006. Surprisingly small HONO emissions from snow surfaces at Browning Pass, Antarctica. *Atmospheric Chemistry and Physics*, **6**, 2569–2580.

Bindschadler, R. 1998. Monitoring ice sheet behavior from space. *Reviews of Geophysics*, **36**(1), 79–104.

Bintajna, R. S. Jonsson and W. Knap. 1997. The annual cycle of the surface energy balance of Antarctic blue ice. *Journal of Geophysical Research*, **102**(D2), 1867–1881.

Bintanja, R. 1999. On the glaciological, meteorological, and climatological significance of Antarctic blue ice areas, *Reviews of Geophysics*, **37**(3), 337–359.

Bisiaux, M. M., R. Edwards, J. R. McConnell, M. A. J. Curran, T. D. Van Ommen, A. M. Smith, T. A. Neumann, D. R. Pasteris, J. E. Penner, and K. Taylor. 2012. Changes in black carbon deposition to Antarctica from two high-resolution ice core records, 1850–2000 AD. *Atmospheric Chemistry and Physics*, **12**, 4107–4115.

Boening, C., M. Lebsock, F. Landerer and G. Stephens. 2012. Snowfall-driven mass change on the East Antarctic ice sheet. *Geophysical Research Letters*, **39**, L21501, 5 pp.

Bohren, C. F. and B. R. Barkstrom. 1974. Theory of the optical properties of snow. *Journal of Geophysical Research*, **79**(30), 4527–4535.

Boyne, H. S. and D. J. Fisk. 1990. A laboratory comparison of field techniques for measurements of the liquid water fraction of snow. CRREL Special Report 90–3.

Brandt, R. E. and S. G. Warren. 1993. Solar-heating rates and temperature profiles in Antarctic snow and ice, *Journal of Glaciology*, **39**(131), 99–110.

Brandt, R. E. and S. G. Warren. 1997. Temperature measurements and heat transfer in near-surface snow at the South Pole, *Journal of Glaciology*, **43**, 339–351.

Carrol, J. J. 1982. Long-term means and short-term variability of the surface energy balance components at the South Pole. *Journal of Geophysical Research*, **87**(C6), 4277–4286.

Choudhury, B. J. and A. T. C. Chang. 1981. The albedo of snow for partially cloudy sky, *Boundary Layer Meteorology*, **20**, 371–389.

Colbeck, S. C. 1982. An Overview of Seasonal Snow Metamorphism. *Reviews of Geophysics and Space Physics*, **20**(1), 45–61.

Colbeck, S., E. Akitaya, R. Armstrong, H. Gubler, J. Lafeuille, K. Lied, D. McClung and E. Morris. 1990. The international classification for seasonal snow on the ground. Wallingford, Oxon, International Association of Scientific Hydrology. International Commission on Snow and Ice.

Domine, F., M. Albert, T. Huthwelker, H.-W. Jacobi, A. A. Kokhanovsky, M. Lehning, G. Picard, W. R. Simpson. 2008. Snow physics as relevant to snow photochemistry. *Atmospheric Chemistry and Physics*, **8**(2), 208.

Fedorov, K. N. and A. I. Ginzburg. 1992. The near-surface layer of the ocean. Utrecht: VSP, 259.

Fierz, C., R. L. Armstrong, Y. Durand, P. Etchevers, E. Greene, D. M. McClung, K. Nishimura, P. K. Satyawali and S. A. Sokratov. 2009. The International Classification for Seasonal Snow on the Ground. *IHP-VII Technical Documents in Hydrology*, **83**, IACS Contribution (1), UNESCO-IHP, Paris.

France, J. L., M. D. King, M. M. Frey, J. Erbland, G. Picard, S. Preunkert, A. MacArthur and J. Savarino. 2011. Snow optical properties at Dome C (Concordia), Antarctica; implications for snow emissions and snow chemistry of reactive nitrogen. *Atmospheric Chemistry and Physics*, **11**, 9787–9801.

Grenfell, T. C., S. G. Warren, and P. C. Mullen. 1994. Reflection of solar radiation by the Antarctic snow surface at ultraviolet, visible, and near-infrared wavelengths. *Journal of Geophysical Research*, **99**, 18669–18684.

Gow, A. J. and R. Rowland. 1965. On the relationship of snow accumulation to surface topography at Byrd Station, Antarctica, *Journal of Glaciology*, **5**(37), 843–847.

Granberg, H. B., P. Cliche, O.-P. Mattila, E. Kanto and M. Leppäranta. 2009. A snow sensor experiment in Dronning Maud Land, Antarctica. *Journal of Glaciology*, **55**(194), 1041–1051.

Gray, J. M. N. T. and L. W. Morland. 1995. The compaction of polar snow packs. *Cold Region Science and Technology*, **23**(1995), 109–119.

Hoffman, M. J., G. A. Catania, T. A. Neumann, L. C. Andrews and J. A. Rumrill. 2011. Links between acceleration, melting, and supraglacial lake drainage of the western Greenland ice sheet. *Journal of Geophysical Research*, 10.1029/2010JF001934.

Holmlund, P. and J.-O. Näslund. 1994. The glacially sculptured landscape in Dronning Maud Land, Antarctica, formed by wet-based mountain glaciation and not by the present ice sheet. *Boreas*, **23**(2), 139–148.

Ingvander, S., I. A.Brown, P. Jansson. 2011. Spatial snow grain size variability along the 126 JASE 2007/2008 traverse route in Dronning Maud Land, Antarctica, and its relation to MOA 127 NDSI index, MEDRIS and MODIS satellite data. ESA Living Planet Symposium Proceedings, Bergen, 128 Norway, 2010. SP-686.

Isaksson, E. 1992. Spatial and temporal patterns in snow accumulation and oxygen isotopes, Western Dronning Maud Land, Antarctica, Report STOU-NG 87, Department of Physical Geography, Stockholm University, Stockholm, Sweden, 86 pp.

Isaksson, E. and W. Karlén. 1994. Spatial and temporal patterns in snow accumulation and oxygen isotopes, Western Dronning Maud Land, Antarctica. *Journal of Glaciology*, **40**(135), 399–409.

Isaksson, E., W. Karlén, N. Gundestrup, P. Mayewski, S. Whitlow and M. Twickler. 1996. A century of accumulation and temperature changes in Dronning Maud Land, Antarctica, *Journal of Geophysical Research*, **101**(D3), 7085–7094.

Kanto, E. 2006. Snow characteristics in Dronning Maud Land, Antarctica, PhD thesis. *Report series in Geophysics*, **49**, Department of Physics, University of Helsinki.

Kärkäs, E., H. B Granberg, C. Lavoie, K. Kanto, K. Rasmus and M. Leppäranta. 2002. Physical properties of the seasonal snow cover in Dronning Maud Land, East-Antarctica. *Annals of Glaciology*, **34**, 89–94.

Kärkäs, E. 2004. Meteorological conditions of the Basen Nunatak in western Dronning Maud Land, Antarctica, during the years 1989-2001. *Geophysica*, **40**(1–2), 39–52.

Keskitalo, J., M. Leppäranta and L. Arvola. 2013. First records on primary producers of epiglacial and supraglacial lakes lakes in the western Dronning Maud Land, Antarctica. *Polar Biology*, in press.

King, J. C. and W. M. Turner. 1997. Antarctic meteorology and climatology. Cambridge University Press, New York, 409 pp.

Kojima, K. 1964. Densification of snow in Antarctica. *In* Mellor, M. (ed.) *Antarctic snow and ice studies*. Washington, DC, American Geophysical Union, Antarctic Research Series Vol. 2, 157–218.

Kumai, M. 1976. Identification of nuclei and concentrations of chemical species in snow crystals sampled at the South Pole. *Journal of Atmospheric Sciences*, **33**, 833–841.

LaChapelle, E. R. 1969. Field guide to snow crystals. University of Washington Press, USA, 101 pp.

Lee-Taylor, J. M. and S. Madronich. 2002. Calculation of actinic fluxes with a coupled atmosphere-snow radiative transfer model, *Journal of Geophysical Research*, **107**(D24), 4796.

Legrand, M. and P. Mayewski. 1997. Glaciochemistry of polar ice cores: a review, *Reviews of Geophysics*, **35**(3), 219–243.

Leppäranta, M., M. Tikkanen and J. Virkanen. 2003. Observations of ice impurities in some Finnish lakes. Proceedings of the Estonian Academy of Science. *Chemistry* **52**(2): 59–75.

Leppäranta, M. 2009. Modelling the formation and decay of lake ice. In George, G., ed. The impact of climate change on European lakes. Aquatic Ecology Series, vol. 4. Berlin: Springer, 63–83.

Lesaffre, B., E. Pougatch and E. Martin. 1998. Objective determination of snow-grain characteristics from images. *Annals of Glaciology*, **26**, 112–118.

Liang, Y.-L., W. Colgan, Q. Lv, K. Steffen, W. Abdalati, J. Stroeve, D. Gallaher and N. Bayou. 2012. A decadal investigation of supraglacial lakes in West Greenland using a fully automatic detection and tracking algorithm. *Remote Sensing of Environment*, **123**, 127–138.

Liston, G. E. and E. Elder. 2006. A Distributed Snow-Evolution Modeling System (SnowModel), *Journal of Hydrometeorology*, **3**, 646–659.

Melvold, K., J. O. Hagen, J. F. Pinglot and N. Gundestrup. 1998. Large spatial variations in accumulation rate in Jotulstraumen ice stream, Dronning Maud Land, Antarctica. *Annals of Glaciology*, **27**, 231–238.

Omega. 1992. The temperature handbook. Stamford, CT, Omega Engineering, 28, 1153 pp.

Paterson, W. S. B. 1994. The physics of glaciers, 3rd edition. Tarrytown, New York, Pergamon/Elsevier Science, Inc. 480 pp.

Perovich, D. 1998. The optical properties of sea ice. *In* Leppäranta, M. (ed.) *Physics of ice-covered seas*, Vol. 1, 195–230. Helsinki University Press.

Perovich, D. 2007. Light reflection and transmission by a temperate snow cover. *Journal of Glaciology*, **53**(181), 201–210.

Petrovic, J. J. 2003. Review Mechanical properties of ice and snow. *Journal of Materials Science*, **38**, Issue 1, 1–6.

Petit, J. R., J. Jouzel, D. Raynaud, N. I. Barkov, J.-M. Barnola, I. Basile, M. Bender, J. Chappellaz, M. Davis, G. Delaygue, M. Delmotte, V. M. Kotlyakov, M. Legrand, V. Y. Lipenkov, C. Lorius, L. Pépin, C. Ritz, E. Saltzman and M. Stievenard. 1999. Climate and atmospheric history of the past 420,000 years from the Vostok ice core, Antarctica. *Nature*, **399**(6735), 429–436.

Pirazzini, R. 2004. Surface albedo measurements over Antarctic sites in summer. *Journal of Geophysical Research*, **109**(D20118).

Raghunath, H. M. 2007. Ground water, 3rd ed. New Delhi: New Age International, 520 pp.

Rasmus, K., H. B Granberg, K. Kanto, E. Kärkäs, C. Lavoie and M. Leppäranta. 2003. Seasonal snow in Antarctica. Data report. *Report Series of Geophysics*, **47**, Department of Physics, University of Helsinki, 100 pp.

Rasmus, K. 2009. Snow characteristics in Dronning Maud Land, Antarctica, PhD thesis. *Report series in Geophysics*, **62**, Department of Physics, University of Helsinki.

Reijmer, C. H. 2001. Antarctic meteorology: A study with automatic weather stations. PhD thesis, University of Utrecht, Netherlands.

Reijmer, C. H. and J. Oerlemans. 2002. Temporal and spatial variability of the surface energy balance in Dronning Maud Land, East Antarctica, *Journal of Geophysical Research*, **107**(D24), 4759.

Richardson, C., E. Aarholt, S.-E. Hamran, P. Holmlund and E. Isaksson. 1997. Spatial distribution of snow in western Dronning Maud Land, East Antarctica, mapped by a ground-based snow radar. *Journal Geophysical Research*, **102**(B9), 20,343–20,353.

Richardson-Näslund, C. 2004. Spatial characteristics of snow accumulation in Dronning Maud Land, Antarctica. *Global Planet Change*, **42**, 31–43.

Rignot, E. and R. H. Thomas. 2007. Mass balance of polar ice sheets. *Science*, **297**, 1502–1506.

Riche, F. and M. Schneebeli. 2012. Thermal conductivity of anisotropic snow measured by three independent methods. *The Cryosphere Discussions*, **6**, 1839–1869.

Royer, A., M. DeAngelis and J. R. Petit. 1983. A 30,000 year record of physical and optical properties of microparticles from an East Antarctic ice core and implications for paleoclimate reconstruction models. *Climate Change*, **5**, 381–412.

Rusin, N. P. 1961. Meteorological and radiational regime of Antarctica. Jerusalem, Israel Program for Scientific Translations.

Sihvola, A. and M. Tiuri. 1986. Snow fork for field determination of the density and wetness profiles of a snow pack. *IEEE Transactions on Geoscience and Remote Sensing*, **GE-24**(5), 717–720.

Stephenson, P. J. 1967. Some considerations of snow metamorphism in the Antarctic ice sheet in the light of ice crystal studies. Physics of Snow and Ice proceedings 1(2), Institute of Low Temperature Science, Hokkaido University, 725–740.

Sturm, M., J. Holmgren, M. König, and K. Morris. 1997. The thermal conductivity of seasonal snow. *Journal of Glaciology*, **43**, 26–41.

Tietäväinen, H. and T. Vihma. 2008. Atmospheric moisture budget over Antarctica and the Southern Ocean based on the ERA-40 reanalysis. *International Journal of Climatology*, **28**, 1977–1995.

Van den Broeke, M. R. 2004a. On the role of Antarctica as heat sink for the global atmosphere. *Journal de Physique IV*, **121**, 115–124.

Van den Broeke, M. R., C. H. Reijmer and R. S. W. Van de Wal. 2004b. A study of the surface mass balance in Dronning Maud Land, Antarctica, using automatic weather stations. *Journal of Glaciology*, **50**(171), 565–582.

Van den Broeke, M. R., C. H. Reijmer, D. Van As, R. S. W. Van de Wal and J. Oerlemans. 2005. Seasonal cycles of Antarctic surface energy balance from automatic weather stations. *Annals of Glaciology*, **41**(1), 131–139.

Van den Broeke, M. R., C. H. Reijmer, D. Van As and W. Boot. 2006. Daily cycle of the surface energy balance in Antarctica and the infuence of clouds. *International Journal of Climatology*, **26**, 1587–1605.

Van Lipzig, N. P. M., E. Van Meijgaard and J. Oerlemans. 2002a. The effect of temporal variations in the surface mass balance and temperature inversion strength on the interpretation of ice-core signals. *Journal of Glaciology*, **48**(63), 611–621.

Van Lipzig, N. P. M., E. Van Meijgaard and J. Oerlemans. 2002b. The spatial and temporal variability of the surface mass balance in Antarctica: Results from a regional climate model. *International Journal of Climatology*, **22**, 1197–1217.

Vehviläinen, J. 2010. Snow modeling on Tellbreen, Svalbard with snowpack snow physical model during winter and spring 2009. *Report Series of Geophysics*, **65**, Department of Physics, University of Helsinki. 81 pp.

Vihma, T., O.-P. Mattila, R. Pirazzini and M. M. Johansson. 2011. Spatial and temporal variability in summer snow pack in Dronning Maud Land, Antarctica. *The Cryosphere*, **5**, 187–201.

Warren, S. G. and W. J. Wiscombe. 1980. A model for the spectral albedo of snow. II. Snow containing atmospheric aerosols. *Journal of the Atmospheric Sciences*, **37**(12), 2734–2745.

Warren, S. G. 1982. Optical properties of snow. *Reviews of Geophysics and Space Physics*, **20**(1), 67–89.

Warren, S. G. and A. D. Clarke, A. D. 1990. Soot in the atmosphere and snow surface of Antarctica, *Journal of Geophysical Research*, **95**, 1811–1816.

Warren, S. G., R. E. Brant and T. C. Grenfell. 2006. Visible and near-ultraviolet absorption spectrum of ice from transmission of solar radiation into snow. *Applied Optics*, **45**(21), 5320–5334.

Warren, S. G., and R. E. Brandt. 2008. Optical constants of ice from the ultraviolet to the microwave: A revised compilation, *Journal of Geophysical Research*, **113**, D14220.

Winther, J.-G., H. Elvehøy, C. E. Bøggild, K. Sand and G. Liston. 1996. Melting, runoff and the formation of frozen lakes in a mixed snow and blue-ice field in Dronning Maud Land, Antarctica. *Journal of Glaciology*, **42**(141), 271–278.

Wiscombe, W. J. 1980. Improved Mie scattering algorithms. Applied Optics, **19**(9), 1505–1509.

Wiscombe, W. J. and S. G. Warren. 1980. A Model for the Spectral Albedo of Snow, I: Pure Snow. *Journal of the Atmospheric Sciences*, **37**, 2712–2733.

Zubov, N. N. 1945. L'dy Arktiki. Moscow: Izdatel'stvo Glavsermorputi, 360 pp. [Arctic ice].